



River signature over coastal area (Eastern Mediterranean): Grain size and geochemical analyses of sediments

Myriam Ghsoub, Milad Fakhri, Thierry Courp, Gaby Khalaf, Roselyne Buscail,
Wolfgang Ludwig

► To cite this version:

Myriam Ghsoub, Milad Fakhri, Thierry Courp, Gaby Khalaf, Roselyne Buscail, et al.. River signature over coastal area (Eastern Mediterranean): Grain size and geochemical analyses of sediments. *Regional Studies in Marine Science*, 2020, 35, pp.101169 -. <10.1016/j.rsma.2020.101169>. <hal-03490089>

HAL Id: hal-03490089

<https://hal.science/hal-03490089v1>

Submitted on 22 Aug 2022

HAL is a multi-disciplinary open access archive for the deposit and dissemination of scientific research documents, whether they are published or not. The documents may come from teaching and research institutions in France or abroad, or from public or private research centers.

L'archive ouverte pluridisciplinaire **HAL**, est destinée au dépôt et à la diffusion de documents scientifiques de niveau recherche, publiés ou non, émanant des établissements d'enseignement et de recherche français ou étrangers, des laboratoires publics ou privés.



Distributed under a Creative Commons CC BY-NC 4.0 - Attribution - Non-commercial use - International License

River signature over coastal area (Eastern Mediterranean):

Grain size and geochemical analyses of sediments

Myriam Ghsoub ^(a, b), Milad Fakhri ^(a), Thierry Courp ^(b), Gaby Khalaf ^(a), Roselyne Buscail ^(b), and Wolfgang Ludwig ^(b)

^(a) Lebanese National Council for Scientific Research – National Centre for Marine Sciences (CNRS-L/CNSM) Lebanon (bihar@cnrs.edu.lb),

^(b) Université de Perpignan Via Domitia, Centre de Formation et de Recherche sur les Environnements Méditerranéens, UMR 5110, 52 Avenue Paul Alduy, 66860, Perpignan, France (cefrem@univ-perp.fr)

Abstract

Rivers and coastal areas are two ecosystems in permanent interaction. Thus, to understand the process occurring at the land-sea continuum, the determination of the origin and fate of sediment and its associated organic matter is critical. Moreover, tracing the source of particulate matter from terrestrial origin has not been adequately carried out in the eastern Mediterranean basin, especially in Lebanon. In order to differentiate between the terrestrial and marine sources of particulate matter and characterize the depositional environments, grain size composition, organic carbon (OC), total nitrogen (TN), Isotopic Ratio ($\delta^{13}\text{C}$), the terrestrial and labile fractions of organic matter, as well as, photosynthetic pigments were analyzed for surface sediment samples collected from the coastal marine area facing the mouth of Ibrahim river and from the river watershed.

This study shows that the combined use of the grain size composition of sediments and carbon isotopic signatures ($\delta^{13}\text{C}$) of its associated organic matter is an efficient tool to track the source and fate of organic matter in highly dynamic estuarine and coastal ecosystems.

The obtained results illustrate the occurrence of two grain size compositional types associated with two different depositional environments. Shallow stations (≤ 30 m) are characterized by a hydrological sorting and strong hydrodynamic conditions leading to the winnowing of the finer fraction to deep stations (≥ 60 m) found to be impacted by river inputs.

Organic carbon and total nitrogen values are strongly correlated with the mud fraction controlling their distribution, and therefore leading to their accumulation in the sediment of deep stations (≥ 60 m). On the other hand, $\delta^{13}\text{C}$ values and terrestrial fraction percentage suggest the

occurrence of riverine materials at the stations (≥ 60 m), while at the shallow stations, addition of local autochthonous production materials occurs associated with high values of chlorophyll and labile organic matter fraction.

Keywords: Eastern Mediterranean, Estuary, Sediments, Grain size, $\delta^{13}\text{C}$ isotopic ratio, Organic carbon.

1. Introduction

Coastal areas are dynamic zones where interaction occurs between land, air and water. Due to the instability at these transitional areas, sediment characteristics are significantly varying from those occurring offshore. In fact, this instability in the environmental conditions that is controlled by waves and currents affects the composition of sediments and its associated parameters, as well as, their distribution and dispersal (Kulkarni et al., 2015).

Coastal sediments generally consist of organic and inorganic particles that reach the coastal zone by different pathways. Particle size analysis is widely applied in environmental studies and used to reveal the origin of sediments, as well as, their deposition and transport mechanisms. In fact, the particle size composition of sediments is closely related to the energetic and hydrodynamic conditions governing the depositional environments (Zhong et al., 2017), since each environment is described by its own particle size characteristics (Baiyegunhi et al., 2017). Particle size distribution is also influenced by several factors such as particle origin, climatic conditions and topography (Abuodha, 2003).

Furthermore, organic matter in all its aspects plays a central role in marine ecosystems as a potential food resource (Fabiano and Danovaro, 1994). Its concentration in surface sediments reflects the amount of food available to the benthic communities. It is affected by sediment characteristics, especially grain size, and it is divided into two fractions: a refractory fraction and a labile fraction. Therefore, in order to estimate the amount of available organic matter for benthic

1 consumers, biochemical classes (lipids, proteins and carbohydrates) must be analyzed since the
2 quantity of organic matter evaluated by the amount of total organic carbon is considered as an
3 overestimation of food availability. During the transport of organic matter from shallower to deeper
4 waters, its labile fraction decreases due to mineralization while the refractory part remains
5 present. Thus, at deeper marine areas acting as depositional environments, organic matter is
6 mainly composed of a refractory fraction (Incera et al., 2003; Winogradow and Pempkowiak,
7 2018).

8 Those organic compounds may derive from marine and freshwater plankton and benthos, as well
9 as, terrestrial matter transported by rivers. Therefore, in order to reveal the origin of organic
10 matter, the $\delta^{13}\text{C}$ isotopic ratio may be analyzed and the contribution of each source may be
11 estimated (Li et al., 2016). In addition, terrestrial organic matter is characterized by more depleted
12 $\delta^{13}\text{C}$ (with a typical range of : -25 to -33‰) than marine organic matter (with a typical range of : -
13 18 to -22‰) (Ranjan et al., 2011; Li et al., 2016; Winogradow and Pempkowiak, 2018). In order
14 to assess the proportions of terrestrial organic carbon in surface marine sediments, a $\delta^{13}\text{C}$ two
15 end-member model may be applied based on the assumption of $\delta^{13}\text{C}$ values for terrestrial and
16 marine end-member carbon (Liu et al., 2015; Li et al., 2016).

17 At marine areas, organic matter is well preserved in the low energy environments associated to
18 finer grain size fractions while primary production occurs at shallow areas near the shoreline
19 characterized by higher nutrient inputs and strong hydrodynamic conditions. Hence, as an
20 important indicator of primary production, chlorophyll-a concentrations may be analyzed
21 (Winogradow and Pempkowiak, 2018; Zhang and Blomquist, 2018). In fact, the analysis of
22 photosynthetic pigments is used to study microphytobenthos communities, particularly in surface
23 layers where photosynthesis occurs and therefore, where marine productivity can be estimated
24 (Magni et al., 2000).

Several studies are carried out worldwide at the land-sea continuum focusing on grain size and geochemical analysis (Mohan, 2000 ; Rajganapathi et al., 2013; Kulkarni et al., 2015; Ramesh et al., 2015 ; Abballe and Chivas, 2017 ; Padhi et al., 2017; Zhong et al., 2017; Wang et al., 2018 ; Winogradow and Pempkowiak, 2018) and in the western Mediterranean, specifically at the Gulf of Lion (Higuera, 2014 ; Pruski et al., 2019). Fewer studies are conducted in the eastern Mediterranean namely at the Greek (Karageorgis et al., 2000) and Lebanese coasts (Fakhri et al., 2008 ; 2018). Indeed, the majority of the studies focused on the watersheds of the Lebanese coastal rivers: El Kabir River by Thomas et al., (2005), El Bared River by Khalaf et al., (2009), al Jaouz River by Nakhlé, (2003) and Khalaf et al., (2007), Antelias River by Saad et al., (2004a) and among the southern coastal rivers: Damour and Awali Rivers by Saad et al., (2004b), Hasbani-Wazzani River by Tarabay, (2011) and the longest Lebanese river, Litani River by Nehme et al., (2014) and Mcheik et al., (2015). Furthermore, several studies were executed on the Ibrahim River watershed by Khalaf, (1984); Korfali and Davies, (2003); Nakhlé, (2003); Assaker, (2016) and El Najjar et al., (2019).

Being one of the largest Lebanese coastal rivers, characterized by the highest flow among the Lebanese rivers (408 million m³/ year) (Fitzpatrick et al., 2001 ; Assaker, 2016), it will be relevant and interesting to choose the Ibrahim River as a case study in order to estimate the sediment inputs and river contribution in the marine environment.

Thus, this study aims to investigate the sediment characteristics and dispersal, as well as, the associated organic matter distribution and sources at the coastal zone facing Ibrahim River Mouth (North of Beirut, Lebanon). It acts as a case study of the eastern Mediterranean basin where studies using a combination of grain size composition of sediments and bulk properties of organic matter including the carbon isotopic ratio ($\delta^{13}\text{C}$) are limited. However, due to the complexity of the coastal environment characteristics, such multiple approaches combining granulometric and geochemical analyses are important.

2. Material and Methods

2.1. Area of study

Located in the eastern Mediterranean basin, at the base of Mount Lebanon chain, the Lebanese coastline (220 km) is characterized by a narrow continental shelf with an average width of 3-5 Km and an average depth of 20-40 m (Emery et al., 1966; Goedicke, 1973). Being parallel to Mount Lebanon, the continental shelf is oriented from the southwest to northeast and its western limit is defined by a strong slope at 100-200 m. As part of the warmest basin of the Mediterranean, the Lebanese coast is governed by a Mediterranean climate marked by two distinct seasons: a smooth winter and a hot and long dry summer promoting the precipitation of carbonates (Sanlaville, 1977).

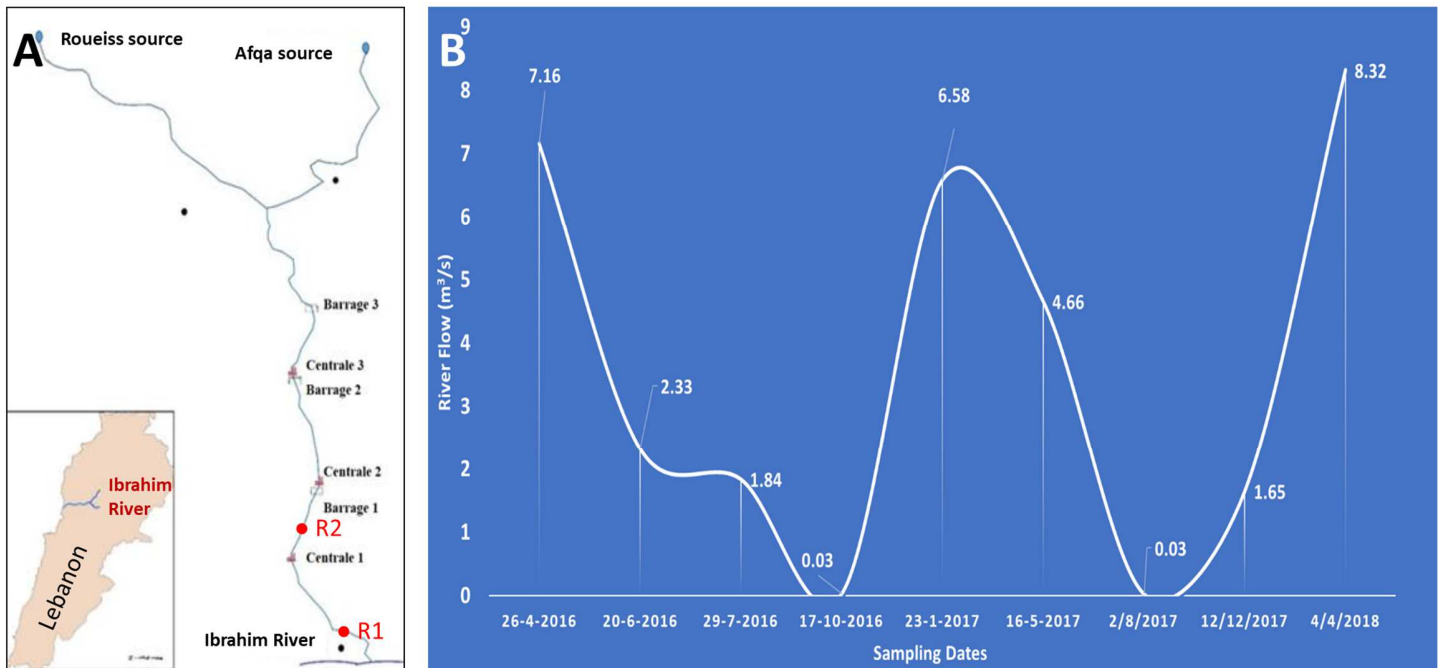
Over coastal areas, wind and currents are two main factors affecting the dispersion of suspended particles and bed sediments. Along the Lebanese coast, the prevailing winds are those of the western sector (southwest or northwest) (Abboud-Abi Saab, 1985). Open and unsheltered, the Lebanese coast is subjected to the prevailing winds and swell. Even in calm weather, a regular swell characterizes Lebanese surface waters especially observed in summer, and during winter the brutal and violent wave action activates the mechanical erosions of the coast (Nakhlé, 2003). The general circulation of surface waters along the Lebanese coast is South-North and the local coastal currents would be considered as simple ramifications of the general offshore currents, running perpendicularly to the coastline, toward the east in an anticyclonic circulation, and being affected by the topography of the continental shelf (Goedicke, 1973).

Small perennial coastal rivers discharge into the sea all along the coast with varying amplitudes affected by seasons and the geomorphology of the coastal zone (Abboud-Abi Saab et al., 2012). Furthermore, several submarine canyons are identified as extensions of valleys and continental rivers between Beirut and Batroun, such as, at the studied coastal area in front of the Ibrahim

1 River (Figure 2). These canyons are usually nearshore in the narrow continental shelf, thus,
2 considered as traps for terrestrial particles, being directly transported to 1500 m (Elias, 2006).

3 Nowadays, the Lebanese coastal zone is subject to overexploitation and several sources of
4 pollution, such as, industrial, agricultural and residential effluents, or other anthropogenic
5 activities. In fact, 4 commercial ports, 15 fishing harbors, dozens of sea pipelines and various
6 industries are located along the Lebanese shoreline. Moreover, about 53 wastewater outfalls are
7 identified along the Lebanese coast which extend only a couple of meters or terminate at the
8 water surface. The Lebanese shoreline is also affected by dumpsites and landfills near big cities
9 such as Dora and Borj Hammoud, Tripoli, Sidon, and Tyre. These dumpsites destroy the coastal
10 ecosystems by spreading solid wastes over the surface water and sea bottom
11 (MOE/UNDP/ECODIT, 2011).

12 Ibrahim River, also known as the Adonis River, is a Lebanese coastal river with two main sources:
13 El Roueiss at 1300 m altitude and Afqa at 1200 m altitude. This river (27 km long) flows into the
14 sea 25 km north of Beirut draining a watershed with accentuated relief. It is characterized by a
15 torrential regime, higher flow occurring between January and June (rainy period), and can be
16 divided into three parts with different slope values: 14% at the upper part, 3% at the intermediate
17 one and 2.5% at the lower part. Ibrahim River is interrupted by three dams that feed three
18 hydroelectric power stations along its watercourse. Water is channeled from one dam to another
19 affecting river flow (Figure 1 A). The catchment area is 326 Km². It includes agricultural lands and
20 is dominated by permeable limestone (Khalaf, 1984). The mean annual flow of Ibrahim River from
21 September 1991 to August 2012 was 10,88 m³/s (Assaker, 2016). It decreased to 5.396 m³/s
22 from September 2015 to August 2016 then increased to 8.758 m³/s from September 2016 to
23 August 2017. The river flow during each sampling date is summarized in Figure 1 B.



2 **Figure 1:** Ibrahim River watershed and Dams

4 Ibrahim River flow during sampling dates (**B**)

3 location (Khalaf, 1984) (**A**)

5 **2.2. Sampling**

6 Nine sampling campaigns were conducted at the coastal marine area facing Ibrahim River mouth
 7 using the platform of the Lebanese scientific vessel “CANA-CNRS”. Sediment samples were
 8 collected for two years from April 2016 to April 2018 (Figure 2) following three sampling transects
 9 (Table 1 and Figure 2) (a southern transect: S; a middle transect: M; and a northern transect: N),
 10 at seven different depths (10, 20, 30, 60, 100, 150, and 200 m), in total 11 stations, using a Van-
 11 Veen grab and PVC corers. The upper 1 cm sediment layer was preserved and transferred into
 12 pre-cleaned glass containers for organic analysis and plastic ones for chemical analysis.
 13 Sediment samples were also collected from the river mouth (R1) and from the packed sediment
 14 at the first dam (R2) (Figure 1 A).

1 **Table 1:** Description of the sampling stations (Depth and geographic location).

| Description | Stations | Depth | Transect | Coordinates |
|---------------------------------|----------|-------|----------|------------------------------|
| Marine surface sediment samples | M1 | 10 m | Middle | 34.06390 ° N 35.63887 ° E |
| | M2 | 20 m | Middle | 34.06398 ° N 35.63520 ° E |
| | M3 | 30 m | Middle | 34.06393 ° N 35.63298 ° E |
| | M6 | 60 m | Middle | 34.06416 ° N 35.62949 ° E |
| | M100 | 100 m | Middle | 34.06548 ° N 35.62020 ° E |
| | M150 | 150 m | Middle | 34.06493 ° N 35.61993 ° E |
| | M200 | 200 m | Middle | 34.06355 ° N 35.61992 ° E |
| | N2 | 20 m | Northern | 34.06878 ° N 35.63568 ° E |
| | N6 | 60 m | Northern | 34.06786 ° N 35.62531 ° E |
| | S2 | 20 m | Southern | 34.05923 ° N 35.63663 ° E |
| | S6 | 60 m | Southern | 34.06091 ° N 35.63086 ° E |
| River surface sediment samples | R1 | | | 34.06443 ° N 35.64465 ° E |
| | R2 | | | 34.08283 ° N 35.68321 ° E |

2

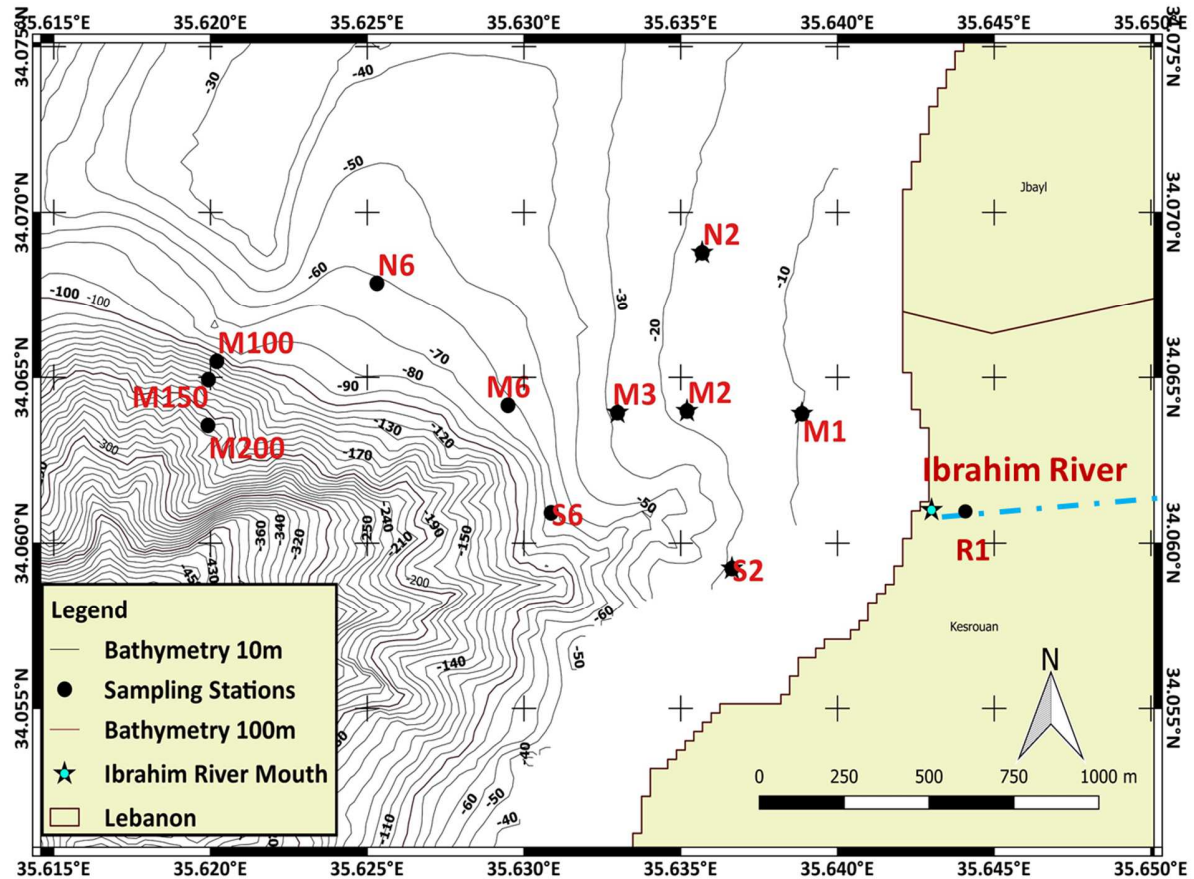


Figure 2: Sampling stations distribution at Ibrahim River coastal marine area.

2.3. Methods of analysis

2.3.1. Grain size analysis:

Particle grain size analysis for sediments less than 2 mm was done using a Laser Scattering Particle Size Distribution Analyzer (Partica LA-950V2) and followed by ultrasonic disaggregation. This machine allows to accomplish the fastest analysis of grain size distribution based on laser diffraction. The range detected by this machine is between 10 nm and 3000 μ m allowing precise measurements.

The results of the grain size composition were processed using the "Gradistat V8.0" Software to calculate statistical parameters (Blott and Pye, 2001). "Triplot" software was used to generate the

trivariate plot. Passega diagram (Passega, 1964) or C-M plot were also used to reveal the hydrodynamic forces governing sediment transport and deposition in the studied area. It consists of plotting “C” (μm): D99 coarser one percentile value and “M” (μm): D50: the median value on a logarithmic scale.

The linear discriminant function (LDF) (Table 2) is a quantitative method usually used to differentiate among different environments and mediums of deposition. This method is based on the fact that each environment of deposition is characterized by its particular energy conditions reflected by the grain size distribution of sediments (Sahu, 1964).

Formulas for mean size (M), variance (r^2), skewness (SK), and kurtosis (KG) deducted from Folk and Ward, (1957) are the most suitable (mutually independent, do not require normal distributions) to be used for this analysis (Sahu, 1964). The average grain size (mean size) of the sediments ($\Phi = -\log_2 d$, d : size (mm)) was calculated and indicated the prevailing energy conditions (Manivel et al., 2016). The standard deviation of the mean (sorting) is a measure of uniformity in the particle size distribution reflecting the fluctuations of the energetic and hydrodynamic conditions governing the deposition medium (Grenier, 2014; Baiyegunhi et al., 2017; Padhi et al., 2017).

Skewness was used to differentiate between symmetrical distribution, the presence of a coarser tail (negative) or finer tail (positive) as an indicator of sub-population mixing (Ramesh et al., 2015; Manivel et al., 2016). Kurtosis was used to evaluate the sorting of the tail in comparison with the center of the curve. The distribution is Leptokurtic when the tail is better sorted in opposition to the Platykurtic distribution. The distribution is Mesokurtic when uniform sorting occurs between the tail and central part.

1 In order to study the total indications of the combined grain size parameters and, thus, reveal the
 2 environment of deposition, a multivariate analysis of sediments granulometry was used based on
 3 the following formulae (Table 2),(Kulkarni et al., 2015; Padhi et al., 2017).

4 **Table 2:** Linear discriminant functions to differentiate among environment of depositions

| Environments and processes discrimination | Equation | Indication |
|---|--|--|
| Between “Aeolian process” and “Littoral environment”: | $Y_1 = -3.5688M + 3.7016r^2 - 2.0766SK + 3.1135KG$ (Eq.1) | $Y_1 > -2.7411$ would indicate littoral environment while $Y_1 < -2.7411$ would refer to an aeolian process. |
| Between “Littoral environment” and “Shallow marine environment”: | $Y_2 = 15.6534M + 65.7091r^2 + 18.1071SK + 18.5043KG$ (Eq.2) | $Y_2 > 63.3650$ would refer to a shallow marine environment while $Y_2 < 63.3650$ would indicate littoral environment. |
| Between “Shallow marine environment” and “Fluvial process”: | $Y_3 = 0.2852M - 8.7604r^2 - 4.8932SK + 0.0428KG$ (Eq.3) | $Y_3 > -7.4190$: would refer to a shallow marine environment while $Y_3 < -7.4190$ would indicate a fluvial process. |
| Between “Fluvial process” and “Turbidity current process” | $Y_4 = 0.7215M - 0.4030r^2 + 6.7322SK + 5.2927KG$ (Eq.4) | $Y_4 < 9.8433$ would indicate turbidity current process and $Y_4 > 9.8433$ would refer to a fluvial process. |

5

6 -To differentiate between “aeolian process” and “littoral environment”, Eq.1 is applied:

7 $Y_1 = -3.5688M + 3.7016r^2 - 2.0766SK + 3.1135KG$ (Eq.1)

8 $Y_1 < -2.7411$ reports an “aeolian process” and $Y_1 > -2.7411$ refers to a “littoral environment”

9 -Eq.2 is applied to distinguish between “Littoral” and “Shallow marine” environments:

10 $Y_2 = 15.6534M + 65.7091r^2 + 18.1071SK + 18.5043KG$ (Eq.2)

11 When Y_2 is < -63.3650 , the environment is “Littoral” and when Y_2 is > -63.3650 , the environment

12 is “shallow marine”.

13 -To discriminate between the “fluvial process” and the “shallow marine environment”, Eq.3 is

14 applied:

15 $Y_3 = 0.2852M - 8.7604r^2 - 4.8932SK + 0.0428KG$ (Eq.3)

16 $Y_3 > -7.4190$ indicates a “shallow marine” environment while $Y_3 < -7.4190$ refers to a “fluvial

17 process”.

-Eq.4 is applied to differentiate between “fluvial” and “turbidity current” deposits:

$$Y_4 = 0.7215M - 0.4030r^2 + 6.7322Sk + 5.2927KG \text{ (Eq.4)}$$

$Y_4 < 9.8433$ refers to “turbidity current” deposits while $Y_4 > 9.8433$ refers to “fluvial” deposits.

Using the discriminant functions, it is then possible to discriminate among processes (aeolian, marine, fluvial, and turbidity current) and environments of deposition (littoral and shallow agitated marine).

Moreover, once those discriminant functions are applied to a sample or population, the environment or process of deposition may be deducted depending on whether the value approaches towards the first side (the first environment) or towards the second side (the second environment) (Sahu, 1964 in Kulkarni et al., 2015 ; Baiyegunhi et al., 2017 ; Padhi et al., 2017).

Prior to the following analysis, sediment samples were crushed using a Planetary Ball Mill PM 200 RETSCH at CEFREM Laboratories.

2.3.2. $\delta^{13}C$ Isotopic Ratio

Samples are decarbonated by repeated additions of HCl (2N), rinsed with cold deionized water before freeze-drying (Schubert and Nielsen, 2000). An elemental analyzer “Eurovector 3000” coupled to a mass spectrometer “Isoprime” (EA-IRMS) was used and the isotopic results are given by the following equation:

$\delta^{13}C = [(R_{\text{sample}}/R_{\text{standard}}) - 1] * 1000$, with $R: {}^{13}C/{}^{12}C$ and the standard is the international Vienna Pee Dee Belemnite (PDB). $\delta^{13}C$ values are reported as per thousand (‰). All samples were analyzed twice and the analytical precision was better than 0.2‰.

A two end-members model of organic matter $\delta^{13}C$ signatures was used to estimate the OC terrestrial fraction (Ft) following this equation (Li et al., 2016):

$$F_t = [(\delta^{13}C_{\text{marine}} - \delta^{13}C_{\text{sample}}) / (\delta^{13}C_{\text{marine}} - \delta^{13}C_{\text{terrestrial}})] * 100 \text{ (Eq.5)}$$

The terrestrial $\delta^{13}\text{C}$ end-member ($\delta^{13}\text{C}_{\text{terrestrial}}$) was chosen based on R1 and R2 values (river stations) -27‰ while the chosen marine end member ($\delta^{13}\text{C}_{\text{marine}}$) -21‰ (ranging from -21.6 to -20.3‰) based on the values taken from marine organism (plankton and benthos) (Li et al., 2016; Wang et al., 2018).

2.3.3. Total Nitrogen (TN)

TN was measured by combustion in an automatic elemental analyzer (Elementar Vario MAX CN).

The calibrations were made with a Soil certified standard. TN was expressed in % of the sample dry weight with a precision of 5 to 10% depending on the concentration.

2.3.4. Organic Carbon (OC)

Total organic carbon was analyzed by adopting the simple titration method approved by the Expertise Centre in Environmental Analysis of Québec (M.A., 2010). OC was expressed in % of the sample dry weight with a precision of 20% and a quantification limit of 0.1%.

2.3.5. Labile Organic matter fraction (LOM)

Carbohydrates (CHO) were measured according to Brink et al. (1960) method at 625 nm (maximum absorbance), and compared to a glucose standard curve. The method of Barnes and Blackstock (1973) was used for the determination of lipids (LPD) at a wavelength of 520 nm, and the concentrations were calculated in comparison to cholesterol standards. Protein (PRT) estimation was accomplished by applying the method of Stevenson and Cheng (1970). The absorbance was read at λ : 570 nm, compared with a L-alanine standard curve.

The labile fraction of organic matter is the sum of CHO, LPD, and PRT. Its proportion was expressed as a percentage of TOC (CLOM/TOC%) after the conversion of CHO, PRT and LPD into carbon equivalents using the conversion factors 0.40, 0.49, and 0.75, respectively (Fabiano and Danovaro, 1994 in Tselepides et al., 2000).

2.3.6. Photosynthetic Pigments

Chlorophyll-*a* and phaeopigments were extracted according to the method described by Lorenzen, (1967) and modified by Magni et al., (2000). The extraction of the photosynthetic pigments was executed by adding 90% acetone to the sample. Spectrophotometric analysis was executed after 24 hours (in dark), before acidification for chlorophyll-*a* and after acidification for phaeopigments.

2.3.7. Statistical Analyses

Statistical analysis was performed using R software. A Schapiro-Wilk test was used to test the normality of the measured variables. A Kruskal Wallis followed by a Dunn-test test were employed to reveal differences between sampling sites and sampling seasons. Moreover, in order to elucidate the relations between the parameters and regroup the sampling stations that share the same characteristics at the studied zone, a principal component analysis was applied.

Principal Component Analysis (PCA) is a multivariate descriptive analysis used to reduce the size of the initial data matrix with a minimum deformation of the reality, in other words, obtain the most relevant summary of the data. Using a correlation matrix, the dispersion of data was analyzed by extracting a reduced number of factors which replaced the initial variables and were used to plot the required distribution graphs to easily understand the data distribution (individuals or stations and variables or studied parameters) (Besse, 1992).

3. Results

3.1. Grain size analysis over Ibrahim River coastal area:

3.1.1. Mean size: An increase of the mean grain size (Φ) was noticed seawards, sandy sediments shifting to silty sediments at deep stations (Figure 3 A). The shallow near shore stations (M1, M2, M3, N2, S2) occurring between 10 and 30 m depth were mainly composed of fine sand

(2-3 phi) as shown by the ternary diagram (Figure 4 A), ranging from 60 to 90%, in opposition to the stations occurring between 60 and 200 m depth mainly constituted of fine fraction (Mud: >4 phi) from 70 to 90% (Stations: M6, N6, S6, M100, M150, M200).

3.1.2. Standard deviation (Sorting): Shallow stations (≤ 30 m) were moderately well to moderately sorted while the deep stations (≥ 60 m) were poorly to very poorly sorted (Figure 3 B).

3.1.3. Skewness: The sediment samples of the studied area followed a symmetrical to very fine skewed distribution (Figure 3 C). At the near shore shallow stations (≤ 30 m), distribution was symmetrical, while at the deep stations (≥ 60 m), distribution was fine to very finely skewed.

3.1.4. Kurtosis: The sediment samples of the studied area were characterized by Mesokurtic to very Leptokurtic distribution indicating the occurrence of one dominant population and another subordinate in the studied region (Ramesh et al., 2015; Manivel et al., 2016).

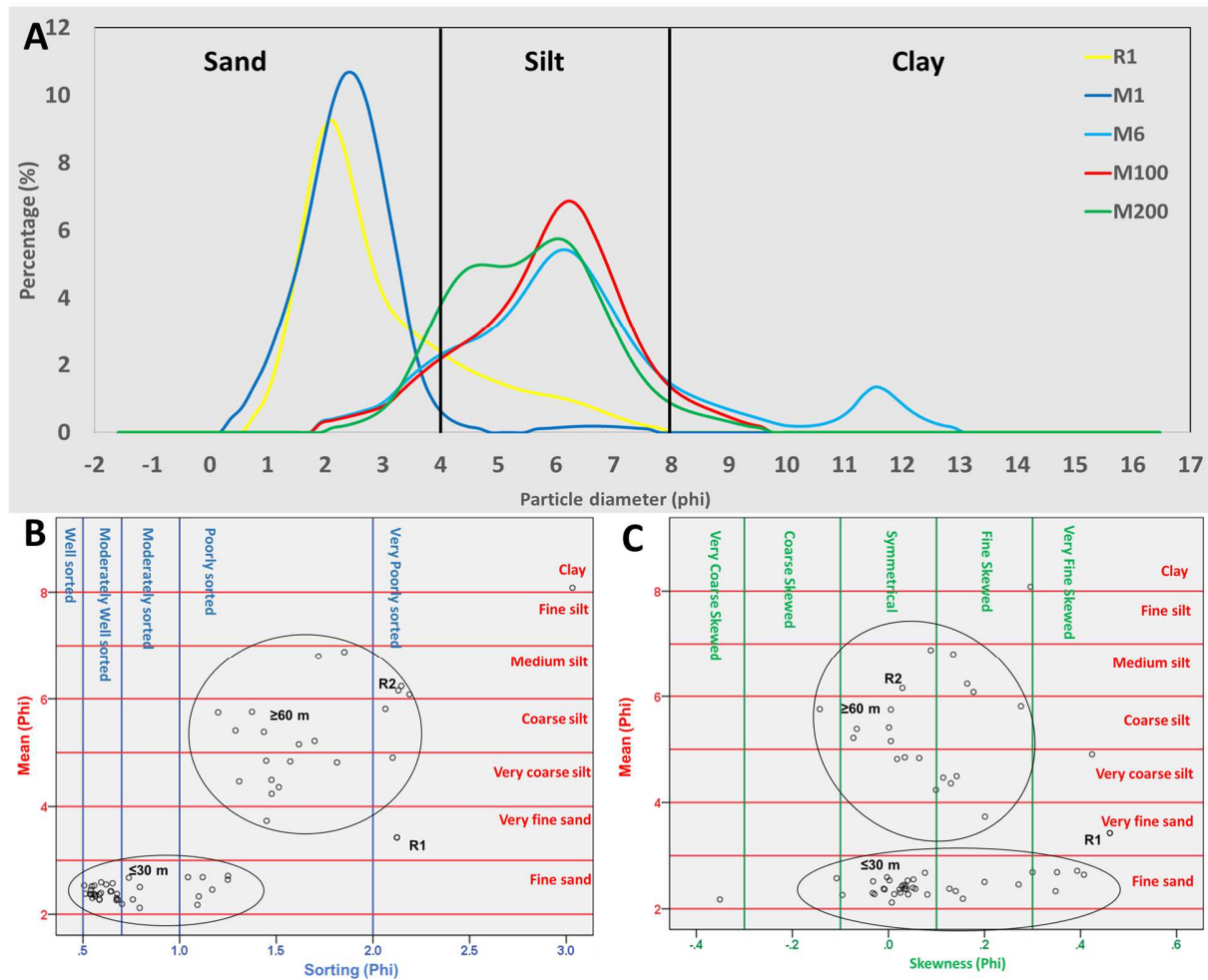
3.1.5. CM Diagram (Passega Diagram):

The CM plot (Figure 4 B) showed the occurrence of two different depositional conditions. Graded and uniform suspension without rolling characterized the deep stations (≥ 60 m), while bottom suspension and rolling characterized the shallow stations (≤ 30 m).

3.1.6. Linear Discriminant Analysis (LDA):

According to Y1 and Y2 respectively, most of the samples belonged to the shallow agitated water environment (Y1) and all the samples fell in the shallow marine condition (Y2) (Figure 5 A). According to Y3, deep stations (≥ 60 m) were characterized by fluvial processes, while shallow stations were characterized by a shallow marine process except for sampling dates: December 2017 and April 2018 (Figure 5 A, B, C). According to Y4, the majority of the samples were attributed to turbidity current deposits in high hydrodynamic environments except for N6 in January 2017 and the sampling dates December 2017 and April 2018 that revealed high river

- 1 flow intensity recorded as fluvial process. These obtained results were verified by the river
- 2 samples which according to both Y3 and Y4, belong to a fluvial environment (Figure 5 B).



- 3
- 4 **Figure 3:** Grain size class weight distribution (A), Mean vs Sorting plot (B), Mean vs Skewness plot (C),
- 5 at the different sampling stations.

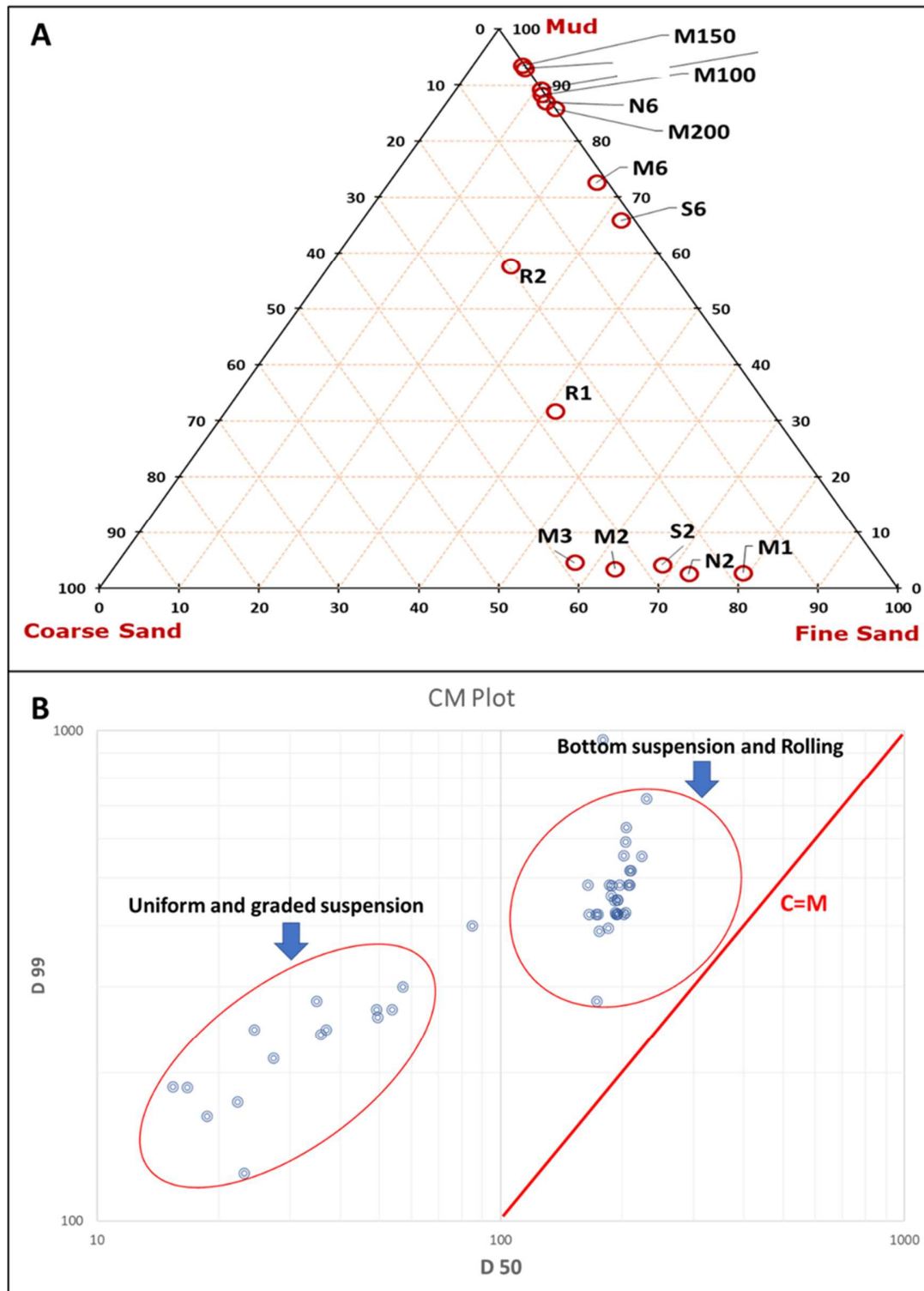
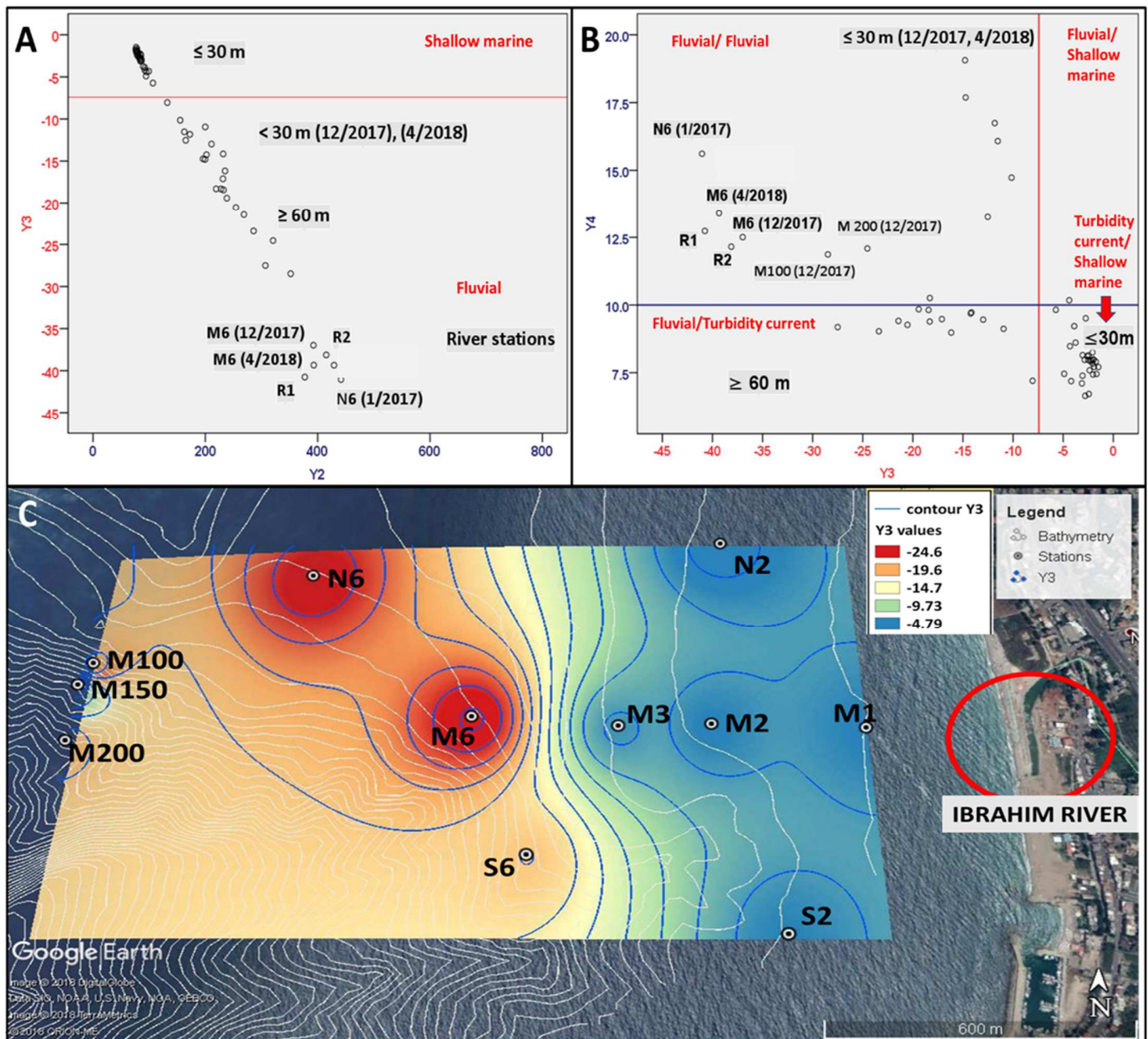


Figure 4: Ternary diagram representing the grain size distribution (A) and the C-M Plot (B) for the sampling stations.



2 **Figure 5:** Linear Discriminate Function (LDF) Plots: Y3 vs Y2 plot (A), Y4 vs Y3 plot (B) and spatial
3 distribution of Y3 (C) at the studied area

4 **3.2. Organic carbon (OC) and total nitrogen (TN) distribution**

5 OC and TN contents (% dry weight) in the surface sediments of Ibrahim River coastal marine area
6 followed similar distributions, characterized by a strong regionality following the distribution of the
7 mud fraction (Figure 6). Low values occurred at shallow stations (≤ 30 m) while high values

1 occurred at deep stations (≥ 60 m). During almost all sampling dates, the lowest OC value of 0.1%
2 occurred mainly at stations M1, M2 and M3 while the highest value, which is approximately 10
3 times greater (1.19%), occurred at the deepest station of 200m (M200).

4 The lowest TN value (0.005%) was recorded at stations M1 and N2 while the highest TN (0.067%)
5 occurred at station S6 in October 2016.

6 **3.3. Photosynthetic pigments and labile organic matter distributions**

7 Chlorophyll-a concentrations were very low and strongly decreasing with depth (Figure 7 A). The
8 highest value of chlorophyll was recorded at station M2 in January 2017, reaching 1.54 $\mu\text{g/g}$ while
9 nearly no values were detected at stations exceeding 100 m depth (M100, M150, M200). The
10 phaeopigment concentrations varied from 0.06 to 4.85 $\mu\text{g/g}$ increasing with depth in opposition to
11 chlorophyll. Concerning labile compounds (Table 3), Σ CHO, LPD, PRT as the sum of biochemical
12 compounds (sugars, lipids and proteins) ranged from 0.525 to 2.671 mg/g. Lipids (0.298 to 1.683
13 mg/g) were the dominant fraction followed by CHO (0.134 to 1.255 mg/g) and PRT (0.029 to 0.418
14 mg/g), which were increasing with depth following the trend of fine fraction, OC, TN, and
15 phaeopigments. Labile organic matter proportions (C-LOM/TOC%) (Figure 7 B) decreased with
16 depth from 38% at the shallow stations (≤ 30 m) to 10% recorded at the deep stations (≥ 60 m).

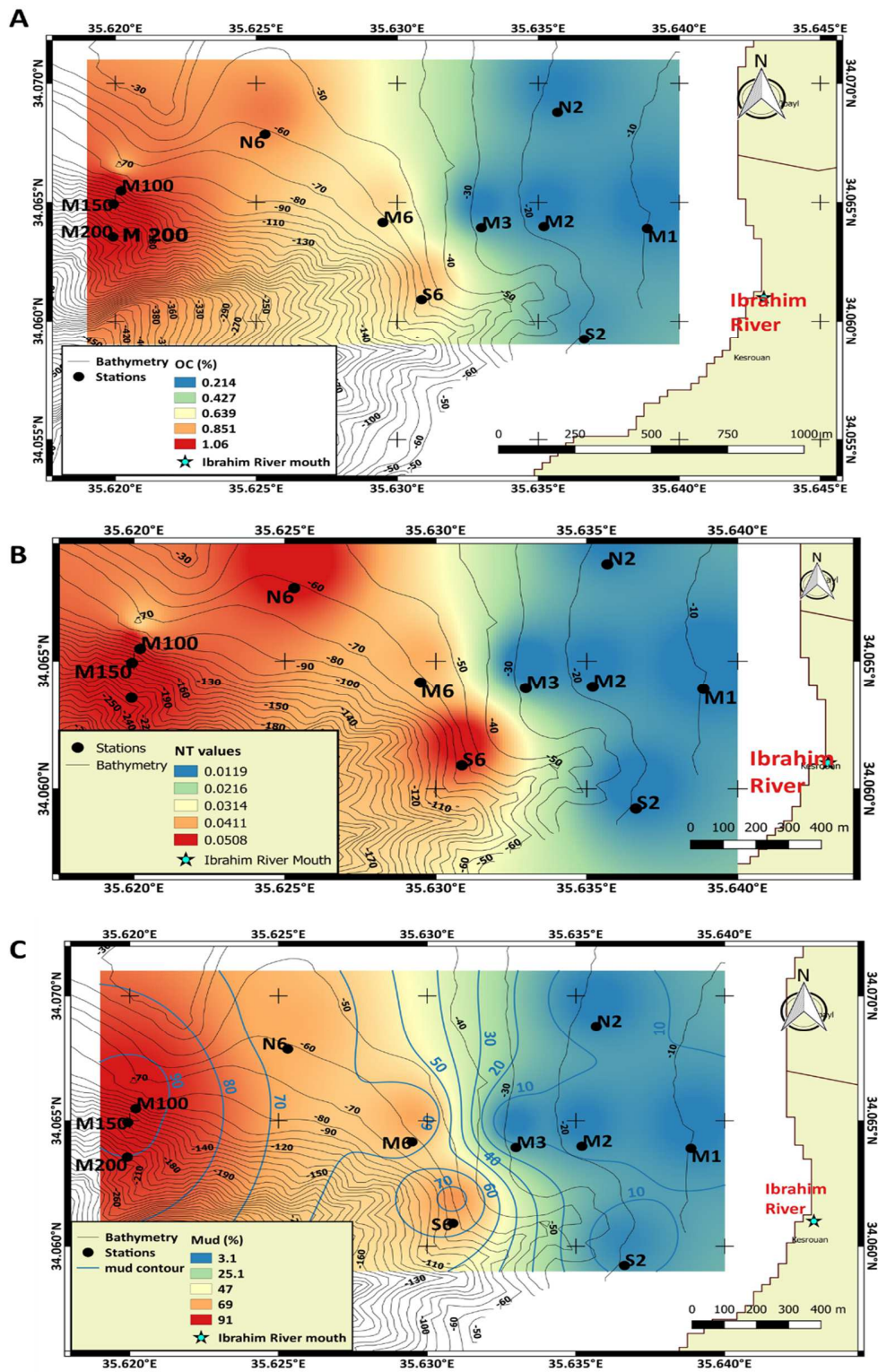


Figure 6: Spatial distribution of organic carbon percentages OC (%) (A), total nitrogen percentages TN (%) (B) and mud fraction percentages (%) (C) at the studied area.

1

2 **Table 3:** Concentrations of geochemical and biochemical studied parameters in the sediments of the
3 studied area

| Stations | TN (%) | OC (%) | CHO (mg/g) | LPD (mg/g) | PRT (mg/g) | Σ (CHO, LPD, PRT) | CLOM (mg/g) | CLOM /TOC % | PRT/CHO |
|----------|--------|--------|------------|------------|------------|--------------------------|-------------|-------------|---------|
| Min | 0.005 | 0.1 | 0.134 | 0.298 | 0.029 | 0.525 | 0.31 | 8 | 0.11 |
| Max | 0.067 | 1.19 | 1.255 | 1.683 | 0.418 | 2.671 | 1.533 | 87 | 0.59 |
| Mean | 0.02 | 0.44 | 0.45 | 0.79 | 0.14 | 1.381 | 0.8 | 27.63 | 0.30 |
| RIVER | | | | | | | | | |
| R1 | 0.03 | 0.54 | 0.92 | 0.62 | 0.18 | 1.72 | 0.89 | 16.66 | 0.2 |
| R2 | 0.12 | 2.10 | 2.81 | 1.24 | 0.76 | 4.81 | 2.36 | 11.24 | 0.27 |

4

5 **3.4. $\delta^{13}\text{C}$ and terrestrial fraction distribution**

6 $\delta^{13}\text{C}$ values ranged from -21.63‰ to -25.27‰ (Figure 8 A). Low values occurred at the deep
7 stations (≥ 60 m). The least negative $\delta^{13}\text{C}$ (-21.63‰) occurred at station M2 in July 2016, while
8 the most negative value (-25.27‰) at station M6 in April 2018.

9

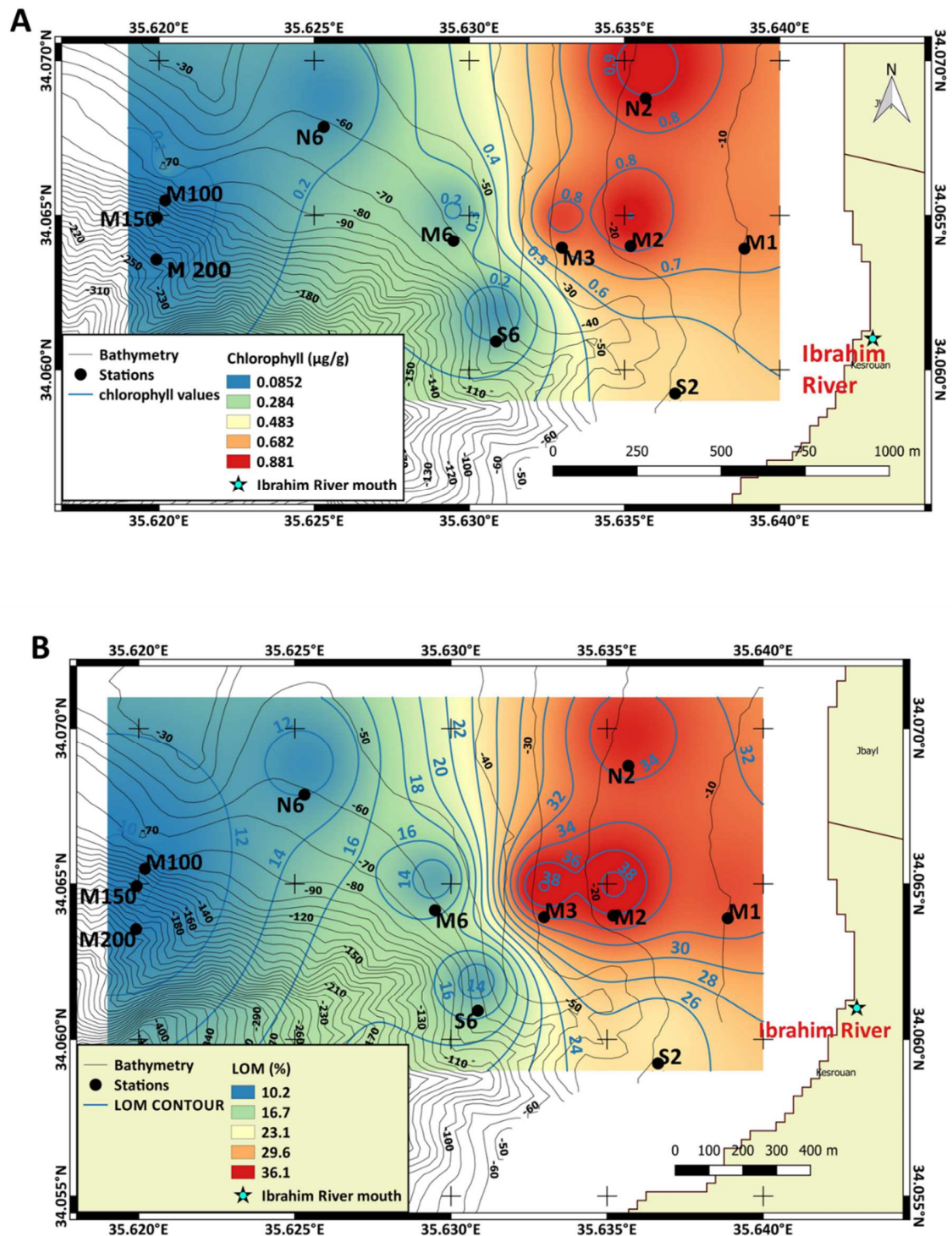


Figure 7: Chlorophyll spatial distribution (A) and labile organic matter percentages (LOM) spatial distribution (B) at the studied area

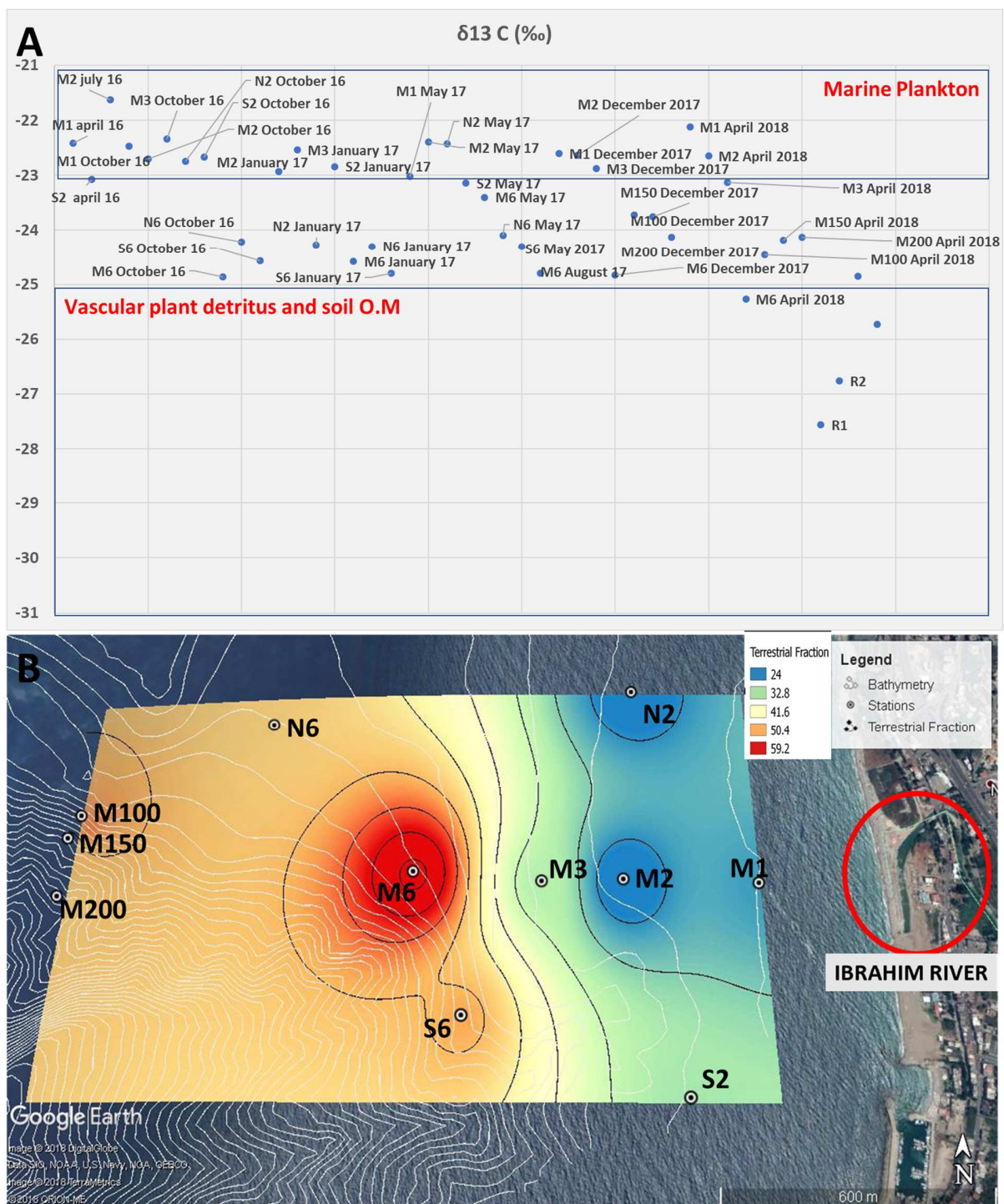


Figure 8: $\delta^{13}\text{C}$ ranges and associated organic matter sources (A) and spatial distribution of the terrestrial fraction (B) at Ibrahim River coastal marine area

The terrestrial fraction percentages (Ft) in the studied area (Figure 8 B) varied between 9.7% at station M2 and 65.7% at station M6 in April 2018. Stations with Ft > 50% dominated by the terrestrial fraction were located off-shore in the depositional area (≥ 60 m) and station N2 (North 20m) in January 2017. Stations with Ft < 50% were located nearshore at stations ≤ 30 m.

4. Discussion

4.1. Environment of depositions revealed by grain size analyses

Continental shelves and specifically open ones usually act as bypass zones characterized by limited sediment supply and strong winnowing (Zhu et al., 2011).

Different types of grain sizes occurring at the studied area with a strong regionality may be the result of sorting due to geomorphology and hydrodynamics. These create different circulation modes associated with different sediment sources. At shallow stations (≤ 30 m), sediments are exposed to wind and waves limiting the accumulation of clay-sized fractions. In fact, the deposition of coarser sediments takes place in high energy environments where resuspension may occur. Finer sediments are transported and deposited in sheltered windless environments, under low energy conditions, acting as depositional areas (≥ 60 m) (Isla et al., 2006; Zhu et al., 2011 ; Manivel et al., 2016; Winogradow and Pempkowiak, 2018). Moreover, at the shallow stations (≤ 30 m), sediments are better sorted and dominated by coarser particles (fine sand), which reflect the occurrence of higher wave energy and strong hydrodynamics. Poorly sorted and finely to very finely skewed distribution characterizing sediments of the deepest stations (≥ 60 m) indicate the addition of finer material from riverine input and the governance of low energy environments allowing the finer fraction to settle down (Manivel et al., 2016; Padhi et al., 2017).

Referring to Stokes's law, coarser particles settle faster than smaller ones. At the shallower sampling points, sediment mainly consists of coarser particles in relation with disturbed conditions: presence of waves and currents preventing the settlement of the finer fraction. At the

1 deeper sampling points, sediments are mainly constituted of finer fraction associated with calmer
2 environments (McComb et al., 1998; Karageorgis et al., 2000). In general, sedimentation is
3 affected by the different energetic and hydrodynamic conditions prevailing at the studied
4 environment. The dominance of coarse size (here fine sand) denotes high energy conditions,
5 whereas the dominance of the fine fraction (here silt) denotes low energy conditions (Amarjouf et
6 al., 2014; Baiyegunhi et al., 2017; Padhi et al., 2017).

7 The case of Ibrahim River presents an originality to what is generally encountered in the rivers
8 generating changes in the size characteristics of the coastal sediments; however, it is similar to
9 the case encountered at the level of another Lebanese seasonal river "Al Jaouz" during a previous
10 study by Fakhri et al., (2008). In fact, in addition to the river input characteristics which supply
11 limited fine fraction due to the presence of the dam, the geomorphology of the coast plays a major
12 role in the effect of the river input. The narrowness of the Lebanese continental shelf promotes
13 the winnowing of the fine fraction offshore (Fakhri et al., 2018).

14 Sediment samples were moderately well sorted to very poorly sorted, thus, marking differences
15 in the uniformity of particle size distribution between stations (Manivel et al., 2016). The negative
16 skewness characterizing sediments of some shallow stations (M1, M2) reveals a loss of finer
17 sediments in high energy environments. The near symmetrical distribution characterizing other
18 shallow stations indicates the mixing of two particle populations generated from two different
19 sources. Thus, the skewness values recorded are strongly affected by wave action prevailing in
20 the studied area. Extremely high Kurtosis values occurring at station S2 and N6 in January 2017,
21 as well as, stations M1, M2 and M3 in December 2017 and April 2018 indicates that part of the
22 sediment is sorted elsewhere in high energy environments (Ramesh et al., 2015; Manivel et al.,
23 2016; Padhi et al., 2017).

24 The combination of all grain size statistical parameters and plots may clearly differentiate between
25 two types of sedimentary environments at the studied area: 1) Shallow stations (≤ 30 m) dominated

by fine sand (coarsest particles) and characterized by the best sorting and a symmetrical distribution transported by rolling and suspension in high energy shallow agitated marine water; 2) Deep stations (≥ 60 m) dominated by silt (finest particles) and characterized by positive skewness and poorly sorted sediments that are transported by uniform graded suspension, settled in low energy environment and considered as fluvial deposits (Kulkarni et al., 2015).

4.2. OC, TN, LOM and photosynthetic pigments spatial distribution

The obtained amounts of OC and TN are associated with each grain size fraction and affected by the hydrodynamic sorting of grain size distribution.

The obtained results are similar to those recorded in front of the Tet coastal river in the north-western basin of the Mediterranean, with annual averages of 0.2% in littoral sands (at 20 m depth) and 0.55% (28 m) in silts and 0.95% in the central mudflat of the continental shelf (at 60-80 m depth) (Pruski et al., 2019). The recorded values may also be compared to those obtained at the east China Sea shelf system facing the Yangtze River, representing low OC (0.1 to 1.3%) and TN (0.005% to 0.14%) values while OC values of (0.1 to 4%) are found in other continental margins reaching 5.9% at the Baltic Sea (Zhu et al., 2011; Winogradow and Pempkowiak, 2018).

OC and TN are significantly correlated with the mud fraction of sediments ($r=0.92$, $p<0.001$, $K=36$ and $r=0.85$, $p<0.001$, $K=36$ respectively) suggesting that the fine fraction (Silt-Clay) is the primary controlling factor of the organic matter concentration in sediments of the studied area.

In fact, the preservation of organic matter is strongly affected by the presence of fine fraction characterized by greater surface area allowing the sorption of organic matter into the clay particles and the aggregation with silt fraction. Furthermore, the strong correlation existing between OC and TN ($r=0.94$, $p<0.001$, $K=36$) may suggest that they share the same origin and that the majority of nitrogen is from organic one (Sondi et al., 2008; Zhu et al., 2011; Li et al., 2016; Abballe and Chivas, 2017; Quiros-Collazos et al., 2017).

1 Carbohydrate values (0.134-1.255 mg/g) were slightly lower than those recorded by Pusceddu et
2 al. (1999) in the sediments of the eastern and western basins of the Mediterranean Sea (1.2-2.4
3 mg/g and 0.9-4.2 mg/g respectively). High concentrations were recorded at 60 m depth in
4 association with high organic carbon concentrations and low photosynthetic pigments. Those
5 results witness the effect of hydrodynamics that governs the coastal zone such as waves, currents
6 and river flow carrying the particles offshore. Moreover, those high concentrations remaining at
7 deep levels may result from the terrestrial origin of carbohydrates. In fact, terrestrial sugars are
8 highly refractive (such as cellulose) while planktonic marine sugars are mainly hydrolysable
9 particles (Fabiano and Pusceddu, 1998).

10 Lipid concentrations (0.298 - 1.683 mg/g) were higher than those recorded in the sediments of
11 the western (0.01-0.66 mg/g) and eastern Mediterranean Sea (0.05-0.19 mg/g) (Fabiano and
12 Pusceddu, 1998), and in the Ligurian Sea (0.02-0.21) (Fabiano et al., 1995; Cividanes et al.,
13 2002). Higher concentrations of lipids are associated with photosynthetic pigment concentrations.
14 Lipids may originate from the decay of plankton, since it is a major constituent of cell membranes.
15 Moreover, high lipid concentrations may also result from the terrestrial and river inputs, as well
16 as, anthropogenic activities in the adjacent land.

17 The concentrations of proteins (0.03 - 0.42 mg/g) were close to those found in the oligotrophic
18 basin of the Ligurian Sea (0.02 - 0.07 mg/g) (Fabiano et al., 1995; Cividanes et al., 2002). The
19 obtained values are considered low when compared to the values recorded at the western
20 Mediterranean Sea (0.5 - 2.6 mg/g) and the Baltic Sea (3.8 - 7.7 mg/g) considered as highly
21 productive basins (Pusceddu et al., 1999; Cividanes et al., 2002).

22 High levels of proteins associated with high organic matter concentrations and finer fraction were
23 measured at deep stations. Shallow sampling points contain less proteins due to active
24 hydrodynamic conditions (Fabiano and Pusceddu, 1998).

1 The mean value of LOM proportion (28% of TOC) is close to those found at highly oligotrophic
2 sites (20% of TOC), and higher than those found at eutrophic ecosystems (3%). Despite the high
3 concentrations of total organic matter at eutrophic sites, the labile fraction increases when
4 proceeding from eutrophic to oligotrophic sites with an increase in food quality (Fabiano et al.,
5 1995).

6 The continental shelf in Lebanon is very narrow; there are no closed bays and water is
7 permanently mixed leading to a fast dispersion of nutrients and pollutants.

8 Moreover, even the stations facing river estuaries in Lebanon are not characterized by high
9 concentrations of chlorophyll, which is probably due to the high prevailing turbidity conditions
10 (instability) and low concentrations of orthophosphates (essential element for the primary
11 production) (Abboud-Abi Saab et al., 2008).

12 **4.3. Seasonal variations of granulometric, geochemical and biochemical parameters**

13 At deep stations (≥ 60 m), seasonal variation was significant for the following parameters: mean
14 grain size, protein, CLOM/TOC, lipids, total nitrogen. For mean grain size, a significant difference
15 existed between dry season (August) and wet season (December, January and April) (p-value:
16 0.015). During the wet season, the highest values were recorded, indicating the addition of fine
17 sediments by fluvial inputs. On the other hand, for proteins, CLOM/TOC, lipids and total nitrogen,
18 the highest values were recorded in the dry season (August and October) showing a significant
19 difference with the wet season (December, January and April). This difference can be attributed
20 to the increase in fluvial inflow during the wet season resulting in a dilution of the labile
21 compounds.

22 At the littoral stations (≤ 30 m), the seasonal difference is significant for the following parameters:
23 mean grain size, sorting, Y3 and Y4, organic carbon, carbohydrates, lipids, labile organic matter
24 (CLOM / TOC), chlorophyll-a and phaeopigments.

For granulometric parameters, a significant difference exists between December and April representative of the wet season and May, June, July, October representative of the dry season. The wet season is characterized by higher values of mean grain size and sorting illustrating the addition of fine sediment by fluvial input, as well as, more negative values of Y3 and Y4, reporting the river environment.

For organic carbon and carbohydrates, the wet season (December and January) is characterized by low values. These compounds were probably transferred with the fine fraction at deep stations. On the other hand, chlorophyll, labile organic matter (CLOM/TOC) and lipids follow almost the same seasonal distributions with the highest values occurring in January 2017.

The highest concentrations of phaeopigments are recorded in June when chlorophyll values are minimal, after the spring bloom, while the lowest values of phaeopigments are recorded for the months of October, January and December.

The highest chlorophyll-*a* concentrations representing the microphytobenthic biomass in the sediments of the studied area were reported in January, July, October and December, while the phytoplankton bloom in Lebanese waters occurs during spring and early summer (June–August) (Abi Saab et al., 2008; Lakkis, 2018). The settlement of photosynthetic cells usually occurs during the first week following the bloom and then, phytoplankton abundance may be insignificant (Fabiano et al., 1995). It is important to mention the opposite trend between the temporal variation of the photosynthetic pigment concentrations in surface sediments (maximum in winter) and in water (maximum in summer), this situation is also reported by Magni and Montani (2006).

Moreover, seasonal variation in the concentrations of photosynthetic pigments is probably affecting the content of labile organic matter in sediments, thus, estimating the effective amount of the bioavailable fraction (Fabiano et al., 1995).

4.4. PRT:CHO ratio and trophic status

1 The PRT: CHO ratio is used to determine the degradation state of organic material in an aquatic
2 ecosystem. In fact, proteins are used more by bacterial organisms than carbohydrates. A low
3 PRT: CHO ratio indicates degraded organic matter while a high ratio indicates new deposited
4 organic material. Usually the dominance of the carbohydrates fraction in the labile organic fraction
5 is considered as an indicator of oligotrophic conditions (Pusceddu et al., 1999).

6 The PRT: CHO ratio (0.11-0.59) appears to be lower than 1 in the sediment of all sampling points.
7 This situation indicates the dominance of degraded material, as well as, the occurrence of
8 terrestrial material. The dominance of carbohydrates over proteins may also indicate a refractory
9 nature of organic matter, associated with high detritus referring to allochthonous and heterotrophic
10 material carried by the river. The ratios found are close to those found in the Ligurian Sea (0.14)
11 and the eastern Mediterranean Sea (0.09), considered as oligotrophic sites, and lower than the
12 values occurring at the Arno estuary (Australia) (0.3-3.6) (Fabiano et al., 1995; Cividanes et al.,
13 2002).

14 The benthic trophic classification may be identified according to the PRT: CHO ratio and labile
15 organic matter concentrations. The sum of labile compounds (Σ CHO, LPD,PRT) ranging from
16 0.525 to 2.671 mg/g is almost similar to the value measured by Fakhri et al., (2008) in the northern
17 Lebanese coastal marine area (0.5-2.5 mg/g). The values of labile compounds represented as C
18 equivalents (CLOM :0.31 to 1.533 mg/g) indicate the prevalence of a meso-oligotrophic status
19 (Pusceddu et al., 2011). Moreover, the PRT concentration is between 0.03 mg/g and 0.42 mg/g,
20 the CHO concentration is between 0.13 mg/g and 1.26 mg/g, and the PRT: CHO ratio is less than
21 1. Therefore, the benthic ecosystem may be considered as meso-oligotrophic to oligotrophic
22 (Dell'Anno et al., 2002).

23 **4.5. Source and degradation degree of the organic matter**

1 Mixed sources of organic matter are revealed by the $\delta^{13}\text{C}$ values. The obtained $\delta^{13}\text{C}$ values are
2 similar to the values recorded at the Yangtze river estuary (-24.5‰ to -21.2‰) but less negative
3 than the values published in the Colville River estuary (-27.1‰ to -25‰) and facing the Amazon
4 River (-24‰ to -27‰) (Li et al., 2016).

5 The two primary origins of organic matter in the studied area may be terrestrial, which is mainly
6 due to the Ibrahim River input, and coastal marine autochthonous. $\delta^{13}\text{C}$ ranges discriminate
7 between marine organic matter from planktonic origin (-21.6‰) in shallow stations (≤ 30 m) and
8 the mixture between terrestrial and marine particles with a dominance of the terrestrial fraction
9 (soil organic matter and vascular plants debris) reaching the deep stations (≥ 60 m) (-23 and -
10 25‰). This reveals a significant input of terrestrial organic carbon transported mainly by the river
11 reaching deep stations and indicates a decrease of planktonic labile fresh organic matter
12 contribution (Li et al., 2016; Abballe and Chivas, 2017; Winogradow and Pempkowiak, 2018).

13 High percentages of allochthonous terrestrial fraction were recorded at the sheltered depositional
14 areas (≥ 60 m) while the shallow exposed areas (≤ 30 m) (strong hydrodynamics) showed low
15 percentage of terrestrial organic matter (Incera et al., 2003).

16 The two variables LOM and Ft are inversely correlated ($r = -0.47$, $p < 0.01$, $K = 36$) (Figure 9 A). The
17 fact that the lability of organic matter decreases with the increase of the terrestrial fraction
18 indicates that fresh labile organic matter originates mainly from marine planktonic origin. High
19 LOM percentages reaching 70% generally occur in shallow nearshore areas (Isla et al., 2006;
20 Wang et al., 2018).

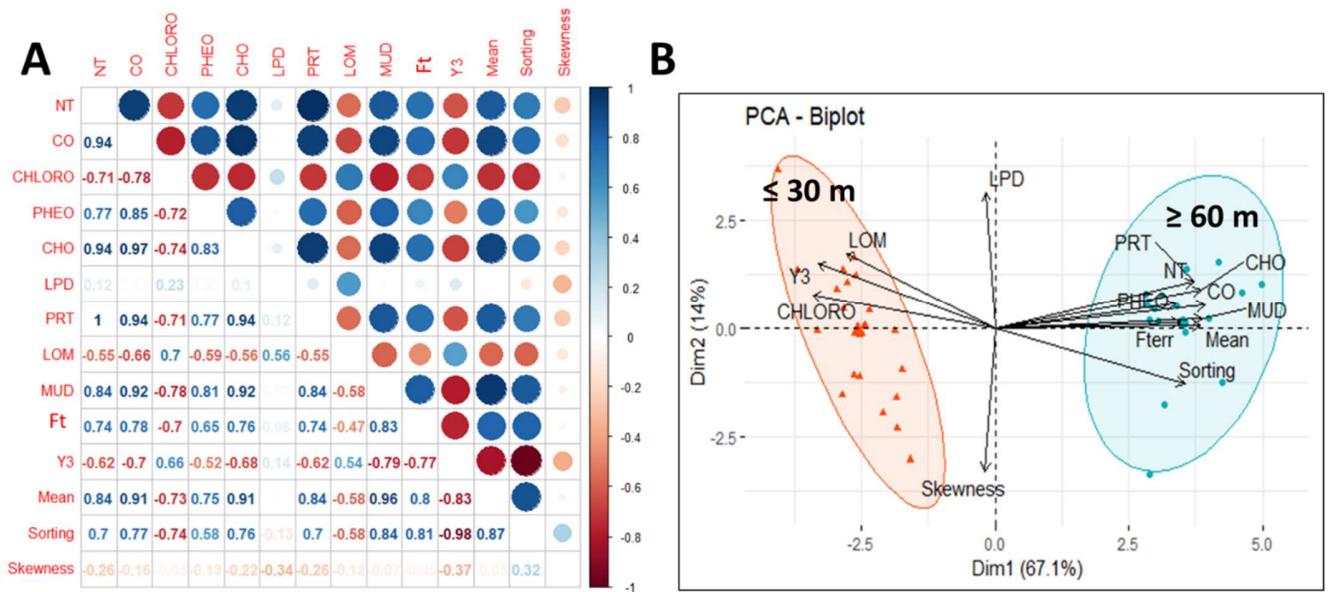


Figure 9: Organic composition and grain size distribution in surface sediments: Correlation Matrix (N=38 K=36 $r=0.324$, $p<0.05$; $r=0.418$, $p<0.01$; $r=0.518$, $p<0.001$) (A)

PCA Biplot: Two components exhibiting 81.1% of the total variance F1 (67.1%) and F2 (14%) distinguishing two groups of parameters associated with two groups of stations according to F1 (B)

A strong correlation was recorded between chlorophyll and food indicators (LOM) ($r=0.7$, $p<0.001$, $K=36$). In fact, high concentrations of labile organic matter and chlorophyll was recorded at the shallower stations (Figure 9 B). This fact may refer to the dominance of the autochthonous marine material issued from the primary production at the shallower stations, as shown by $\delta^{13}\text{C}$ values and the percentage of terrestrial fraction. This is contrary to the case of the Adriatic Sea, facing the Po River, where chlorophyll concentrations in sediment, affected by the river plume, increased from 0.8 to 1.6 $\mu\text{g/g}$ when proceeding off-shore due to the light obstruction of river suspended particles (Dell'Anno et al., 2008; Liu et al., 2015).

Moreover, the difference in grain size distribution among the stations seems to affect the distribution and the degree of degradation of organic matter (Wang et al., 2018). The mud dominated area (≥ 60 m) characterized by silt-clay fraction is associated with a high OC value and a low LOM content. This is reflected through the strong positive correlation occurring between mud and OC ($r=0.92$, $p<0.001$, $K=36$) and TN ($r=0.84$, $p<0.001$, $K=36$), respectively. This is in opposition to the strong negative correlation between mud and LOM ($r=-0.55$, $p<0.001$, $K=36$).

A preservation phenomenon of organic matter in sediments was marked from shallow (≤ 30 m) to deep stations (≥ 60 m) where the refractory organic matter fraction (biochemically resistant) becomes dominant. At these depositional areas, the labile fraction decreases in association with the decrease of the marine planktonic autochthonous contribution and the increase of the terrestrial fraction. Terrestrial organic matter accumulating in marine ecosystems is mainly composed of refractory organic matter while marine autochthonous organic matter from plankton origin is mainly labile and directly mineralized. Higher percentages of refractory organic matter are mainly due to the loss by mineralization of the labile organic matter during the transport of organic matter from near shore (higher energy conditions) to the deepest depositional areas (Winogradow and Pempkowiak, 2018).

The terrestrial fraction deducted from $\delta^{13}\text{C}$ ratio of organic matter differentiates between two types of environments (≤ 30 m and ≥ 60 m) associated with two depositional environments revealed by grain size analyses (Figure 9 B) and verified by the Kruskal Wallis and Dunn test (p value <0.05 for all the variables).

5. Conclusion

The actual research work demonstrates that a combination of both granulometric and organic matter parameters including the carbon isotopic ratio ($\delta^{13}\text{C}$) is able to differentiate between the sources of sediments and its associated organic matter among marine and terrestrial origins using

1 sediment samples collected from the Ibrahim River watershed and its adjacent coastal marine
2 area.

3 The studied area is found to be characterized by two depositional environments associated with
4 two different sources of organic matter, respectively. The high energy nearshore shallow marine
5 area (≤ 30 m) is characterized by sediments that are dominated by fine sand and characterized
6 by low values of organic carbon and total nitrogen. At these sampling points, organic matter is
7 mainly fresh and from marine autochthonous source witnessed by the occurrence of higher LOM
8 percentages and chlorophyll-*a* concentrations. The deep windless low energy marine area (≥ 60
9 m) is characterized by sediments that are dominated by the fine fraction considered as fluvial
10 deposits carried by the Ibrahim River flow and characterized by high OC and TN values. At these
11 sampling points, the organic matter fraction is mainly refractory and from terrestrial allochthonous
12 origin as revealed by the $\delta^{13}\text{C}$ values.

13 Moreover, according to the PRT:CHO ratio and the concentration of labile organic matter, the
14 benthic ecosystem could be considered as meso-oligotrophic to oligotrophic.

15 This study provides an accurate estimation of organic matter origin (marine or terrestrial) and
16 presents a new valuable sediment tracing tool by combining grain size composition of sediments
17 with the carbon isotopic signature ($\delta^{13}\text{C}$) of its associated organic matter. In addition, it is
18 considered as an innovative research work for the coastal eastern Mediterranean Basin, and it
19 could establish a starting point of comparison with numerous other studies conducted along the
20 coastal western Basin.

21 **Acknowledgments**

22 This paper constitutes a part of the PhD of Myriam Ghsoub, supported by the CNRS-L (National
23 Council for Scientific Research-Lebanon) scholarship. The authors would like to thank the
24 NCMS/CNRS-L (National Center for Marine Sciences) and the CEFREM (Centre de Formation

et de Recherche sur les Environnements Méditerranéens UMR 5110 (CNRS France) Université de Perpignan - Via Domitia for hosting this work and providing technical assistance. The authors would also like to thank the Platform for Research and Analysis in Environmental Sciences of the Lebanese University (UL) for grain size analysis.

BIBLIOGRAPHY

- Abballe, P.A., Chivas, A.R., 2017. Organic matter sources, transport, degradation and preservation on a narrow rifted continental margin: Shoalhaven, southeast Australia. *Org. Geochem.* 112, 75–92. <https://doi.org/10.1016/j.orggeochem.2017.07.001>
- Abboud-Abi Saab, M., 1985. Contribution à l'étude des populations microplanctoniques des eaux côtières libanaises (Méditerranée Orientale). Université d'Aix-Marseille II.
- Abboud-Abi Saab, M., Fakhri, M., Kassab, M.-T., Matar, N., 2012. Spatial and vertical influence of river inputs on the marine primary production in Lebanese coastal waters : A case study, in: INOC-CNRS, International Conference on "Land-Sea Interactions in the Coastal Zone." Jounieh-Lebanon, pp. 62–73.
- Abboud-Abi Saab, M., Fakhri, M., Sadek, E., Matar, N., 2008. An Estimate of the Environmental Status of Lebanese Littoral Waters Using Nutrients and Chlorophyll-A as Indicators. *Leban. Sci. J.* 9, 43–60.
- Abuodha, J.O.Z., 2003. Grain size distribution and composition of modern dune and beach sediments, Malindi Bay coast, Kenya. *J. African Earth Sci.* 36, 41–54. [https://doi.org/10.1016/S0899-5362\(03\)00016-2](https://doi.org/10.1016/S0899-5362(03)00016-2)
- Amarjoun, N., Hammadi, A., Oujidi, M., Rezqi, H., 2014. Sedimentological, geochemical and morphoscopic characterization of sediments from Nador Harbor (Morocco). *Bull. l'institut Sci. Rabat, Sect. Sci. la Terre* 36, 1–11.
- Assaker, A., 2016. Hydrologie et Biogéochimie du Bassin Versant du Fleuve Ibrahim : Un Observatoire du Fonctionnement de la Zone Critique au Liban. Institut National Polytechnique de Toulouse (INP Toulouse).
- Baiyegunhi, C., Liu, K., Gwavava, O., 2017. Grain size statistics and depositional pattern of the Eccra Group sandstones, Karoo Supergroup in the Eastern Cape Province, South Africa. *Open Geosci.* 9, 554–576. <https://doi.org/10.1515/geo-2017-0042>
- Barnes, H., Blackstock, J., 1973. Estimation of lipids in marine animals and tissues: detailed investigation of the sulphophosphovanillin method for 'total' lipids. *J. Exp. Mar. Bio. Ecol.* 12, 103–118.
- Besse, P.C., 1992. PCA stability and choice of dimensionality. *Stat. Probab. Lett.* 13, 405–410.
- Blott, S.J., Pye, K., 2001. Gradistat: A grain size distribution and statistics package for the analysis of unconsolidated sediments. *Earth Surf. Process. Landforms* 26, 1237–1248. <https://doi.org/10.1002/esp.261>
- Brink, R., Dubach, P., Lynch, D., 1960. Measurement of Carbohydrates in soil hydrolyzates with Anthrone. *Soil Sci.* 89, 157–166.
- Cividanes, S., Incera, M., Lopez, J., 2002. Temporal variability in the biochemical composition of sedimentary organic matter in an intertidal flat of the Galician coast (NW Spain). *Oceanol. Acta* 25, 1–12.
- Dell'Anno, A., Mei, M.L., Pusceddu, A., Danovaro, R., 2002. Assessing the trophic state and eutrophication of coastal marine systems: A new approach based on the biochemical composition of sediment organic matter. *Mar. Pollut. Bull.* 44, 611–622. [https://doi.org/10.1016/S0025-326X\(01\)00302-2](https://doi.org/10.1016/S0025-326X(01)00302-2)
- Dell'Anno, A., Pusceddu, A., Langone, L., Danovaro, R., 2008. Biochemical composition and early diagenesis of organic matter in coastal sediments of the NW Adriatic Sea influenced by riverine inputs. *Chem. Ecol.* 24, 75–85. <https://doi.org/10.1080/02757540701814580>
- El Najjar, P., Kassouf, A., Probst, A., Probst, J.L., Ouaini, N., Daou, C., El Azzi, D., 2019. High-frequency monitoring of surface water quality at the outlet of the Ibrahim River (Lebanon): A multivariate assessment. *Ecol. Indic.* 104, 13–23. <https://doi.org/10.1016/j.ecolind.2019.04.061>
- Elias, A., 2006. Le chevauchement de Tripoli-Saida: croissance du Mont-Liban et risque sismique. Institut de Physique du Globe de Paris.
- Emery, K.O., Heezen, B.C., Allan, T.O., 1966. Bathymetry of the Eastern Mediterranean sea. *Deep Sea Res.* 13, 173–192.
- Fabiano, M., Danovaro, R., 1994. Composition of organic matter in sediments facing a river estuary (Tyrrhenian Sea): relationships with bacteria and microphytobenthic biomass. *Hydrobiologia* 277, 71–84.

- 1 Fabiano, M., Danovaro, R., Frascchetti, S., 1995. A three-year time series of elemental and biochemical composition of organic
2 matter in subtidal sandy sediments of the Ligurian Sea (northwestern Mediterranean). *Cont. Shelf Res.* 15, 1453–1469.
3 [https://doi.org/10.1016/0278-4343\(94\)00088-5](https://doi.org/10.1016/0278-4343(94)00088-5)
- 4 Fabiano, M., Pusceddu, A., 1998. Total and hydrolysable particulate organic matter (Carbohydrates, proteins, lipids) at a coastal
5 station in Terra Nova Bay (Ross Sea, Antarctica). *Polar Biol* 19, 125–132.
- 6 Fakhri, M., Abboud-Abi Saab, M., Romano, J., 2008a. The use of sediments to assess the impact of Selaata Phosphate Plant on
7 Batroun Coastal area (Lebanon , Levantine Basin). *Leban. Sci. J.* 9, 29–42.
- 8 Fakhri, M., Abboud-Abi Saab, M., Romano, J., Mouawad, R., 2008b. Impact of phosphate factory on the biological characteristics of
9 North Lebanon surface sediments (Levantine Basin) [WWW Document]. <hal-00357034>.
- 10 Fakhri, M., Ghanem, A., Ghsoub, M., Ghaith, A., 2018. Environmental status of the bay of Jounieh through the evaluation of its
11 marine sediments' characteristics. *Leban. Sci. J.* 19, 418–433.
- 12 Fitzpatrick, A., Fox, J., Leung, K., 2001. Environmental Baseline Survey of the Nahr Ibrahim, Lebanon. Massachusetts Institute of
13 Technology, Cambridge.
- 14 Folk, R.L., Ward, W.C., 1957. Brazos River Bar: A Study in the significance of grain size parameters. *J. Sediment. Petrol.* 27, 3–26.
- 15 Goedicke, T.R., 1973. Distribution of surface currents and drift along the central continental shelf of Lebanon as related to pollution.
16 Beyrouth.
- 17 Grenier, J.-F., 2014. Caractérisation pétrographique et pétrophysique du groupe de postdam dans le forage A203, Basses-Terres
18 du Saint Laurent. Québec.
- 19 Higuera, M., 2014. Impact of eastern storm on the transfer of particulate organic matter into the Gulf of Lion (NW Mediterranean
20 Sea). Université de Perpignan Via-Domitia.
- 21 Incera, M., Cividanes, S.P., Lastra, M., López, J., 2003. Temporal and spatial variability of sedimentary organic matter in sandy
22 beaches on the northwest coast of the Iberian Peninsula. *Estuar. Coast. Shelf Sci.* 58, 55–61. [https://doi.org/10.1016/S0272-](https://doi.org/10.1016/S0272-7714(03)00040-4)
23 [7714\(03\)00040-4](https://doi.org/10.1016/S0272-7714(03)00040-4)
- 24 Isla, E., Rossi, S., Palanques, A., Gili, J.M., Gerdes, D., Arntz, W., 2006. Biochemical composition of marine sediment from the
25 eastern Weddell Sea (Antarctica): High nutritive value in a high benthic-biomass environment. *J. Mar. Syst.* 60, 255–267.
26 <https://doi.org/10.1016/j.jmarsys.2006.01.006>
- 27 Karageorgis, A., Anagnostou, C., Sioulas, A., Eleftheriadis, G., Tsirambides, A., 2000. Distribution of surficial sediments in the
28 Southern Evoikos and Petalioi Gulfs, Greece. *Mediterr. Mar. Sci.* 1, 111–122.
29 <https://doi.org/http://dx.doi.org/10.12681/mms.282>
- 30 Khalaf, G., 1984. Contribution à l'étude écologique des fleuves côtiers du Liban : 2- cours moyen et inférieur du Nahr Ibrahim. *Bull.*
31 *Mens. la Société Linnéenne Lyon* 53, 9–20.
- 32 Khalaf, G., Slim, K., Abi Ghanem, C., Nakhlé, K., Fakhri, M., 2009. Caractérisation et corrélation des paramètres biotiques et
33 abiotiques des eaux du Nahr El Bared. *Leban. Sci. J.* 10, 3–21.
- 34 Khalaf, G., Slim, K., Saad, Z., Nakhlé, K.F., 2007. Evaluation de la qualité biologique des eaux du Nahr el Jaouz (Liban) : application
35 des méthodes indicelles. *Bull. Mens. la Société linnéenne Lyon* 76, 255–268. <https://doi.org/10.3406/linly.2007.13667>
- 36 Korfali, S. I. and Davies, B.E., 2003. A comparison of metals in sediments and water in the river Nahr-Ibrahim, Lebanon: 1996 and
37 1999. *Environ. Geochem. Health* 25, 41–50.
- 38 Kulkarni, S.J., Deshbhandari, P.G., Jayappa, K.S., 2015. Seasonal Variation in Textural Characteristics and Sedimentary
39 Environments of Beach Sediments , Karnataka Coast , India. *Aquat. Procedia* 4, 117–124.
40 <https://doi.org/10.1016/j.aqpro.2015.02.017>
- 41 Lakkis, S., 2018. Le phytoplancton des eaux marines libanaises et du bassin levantin. Biologie, Biodiversité, biogéographie, 2nd ed.
42 Publications de l'Université Libanaise.
- 43 Li, Y., Zhang, H., Tu, C., Fu, C., Xue, Y., Luo, Y., 2016. Sources and fate of organic carbon and nitrogen from land to ocean:
44 Identified by coupling stable isotopes with C/N ratio. *Estuar. Coast. Shelf Sci.* 181, 114–122.
45 <https://doi.org/10.1016/j.ecss.2016.08.024>
- 46 Liu, D., Li, X., Emeis, K.C., Wang, Y., Richard, P., 2015. Distribution and sources of organic matter in surface sediments of Bohai
47 Sea near the Yellow River Estuary, China. *Estuar. Coast. Shelf Sci.* 165, 128–136. <https://doi.org/10.1016/j.ecss.2015.09.007>
- 48 Lorenzen, C.J., 1967. Determination of chlorophyll and pheopigments: Spectrophotometric equations. *Limnol. Oceanogr.* 12, 343–
49 3446.
- 50 M.A., 2010. Détermination du carbone organique total dans les solides: dosage par titrage. Québec.

- 1 Magni, P., Abe, N., Montani, S., 2000. Quantification of microphytobenthos biomass in intertidal sediments: layer-dependant
2 variation of chlorophyll-a content determined by spectrophotometric and HPLC methods. *La Mer* 38, 57–63.
- 3 Magni, P., Montani, S., 2006. Seasonal patterns of pore-water nutrients, benthic chlorophyll a and sedimentary AVS in a
4 macrobenthos-rich tidal flat. *Hydrobiologia* 571, 297–311. <https://doi.org/10.1007/s10750-006-0242-9>
- 5 Manivel, T., Mukesh, M., Chandrasekaran, A., Rajmohan, R., Immanuel David, T., Premkumar, R., 2016. Studies on textural
6 characteristics of sediments in Lower Gadilam River, Cuddalore District, Tamilnadu, India. *Int. J. Adv. Res.* 4, 694–705.
- 7 McComb, A.J., Qiu, S., Lukatelich, R.J., McAuliffe, T.F., 1998. Spatial and temporal heterogeneity of sediment phosphorus in the
8 Peel-Harvey Estuarine System. *Estuar. Coast. Shelf Sci.* 47, 561–577. <https://doi.org/10.1006/ecss.1998.0389>
- 9 Mcheik, A., Fakih, M., Trabulsi, H., Toufaily, J., Hamieh, T., Garnier-Zarli, E., Bousserhine, N., 2015. Metal Pollution Assessment of
10 Sediment and Water in Al-Ghadir River: Role of Continuously Released Organic Matter and Carbonate and Their Purification
11 Capacity. *Int. J. Environ. Monit. Anal.* 3, 162–172. <https://doi.org/10.11648/j.ijema.20150303.18>
- 12 MOE/UNDP/ECODIT, 2011. State and trends of the Lebanese environment. Third édition.
- 13 Mohan, P.M., 2000. Sediment transport mechanism in the Vellar estuary, east coast of India. *Indian J. Mar. Sci.* 29, 27–31.
- 14 Nakhlé, K., 2003. Le mercure, le cadmium et le plomb dans les eaux littorales libanaises: apports et suivi au moyen de bio-
15 indicateurs quantitatifs (éponges, bivalves et gastéropodes). Université Paris 7.
- 16 Nehme, N., Haydar, C., Koubaissy, B., Fakih, M., Awad, S., Toufaily, J., Villieras, F., Hamieh, T., 2014. Metal concentrations in river
17 water and bed sediments of the Lower Litani River Bassin, Lebanon. *J. Adv. Chem.* 8, 12p.
- 18 Padhi, D., Singarasubramanian, S.R., Panda, S., Venkatesan, S., 2017. Depositional Mechanism as Revealed from Grain size
19 Measures of Rameswaram Coast, Ramanathapuram District, Tamil Nadu, India. *Int. J. Theor. Appl. Sci.* 9, 168–177.
- 20 Passega, R., 1964. Grain Size Representation by Cm Patterns as a Geological Tool. *J. Sediment. Petrol.* 34, 830–847.
- 21 Pruski, A.M., Buscail, R., Bourrin, F., Vétion, G., 2019. Influence of coastal Mediterranean rivers on the organic matter composition
22 and reactivity of continental shelf sediments: The case of the Têt River (Gulf of Lions, France). *Cont. Shelf Res.* 181, 156–
23 173. <https://doi.org/10.1016/j.csr.2019.05.009>
- 24 Pusceddu, A., Bianchelli, S., Gambi, C., Danovaro, R., 2011. Assessment of benthic trophic status of marine coastal ecosystems :
25 Significance of meiofaunal rare taxa. *Estuar. , Coast. Shelf Sci.* 93, 420–430. <https://doi.org/10.1016/j.ecss.2011.05.012>
- 26 Pusceddu, A., Sara, G., Armeni, M., Fabiano, M., Mazzola, A., 1999. Seasonal and spatial changes in the sediment organic matter
27 of a semi-enclosed marine system (W-Mediterranean Sea). *Hydrobiologia* 397, 59–70.
- 28 Quiros-Collazos, L., Pedrosa-Pàmies, R., Sanchez-Vidal, A., Guillén, J., Duran, R., Cabello, P., 2017. Distribution and sources of
29 organic matter in size-fractionated nearshore sediments off the Barcelona city (NW Mediterranean). *Estuar. , Coast. Shelf*
30 *Sci.* 189, 267–280. <https://doi.org/10.1016/j.ecss.2017.03.004>
- 31 Rajganapathi, V.C., Jitheshkumar, N., Sundararajan, M., Bhat, K.H., Velusamy, S., 2013. Grain size analysis and characterization of
32 sedimentary environment along Thiruchendur coast, Tamilnadu, India. *Arab. J. Geosci.* 6, 4717–4728.
33 <https://doi.org/10.1007/s12517-012-0709-0>
- 34 Ramesh, G., Ramkumar, T., Mukesh, M. V., 2015. A Study on the Textural Characteristics of Arasalar River Estuary Sediments of
35 Karaikal, East Coast of India. *Int. J. Recent Sci. Res.* 6, 2779–2782.
- 36 Ranjan, R.K., Routh, J., Ramanathan, A.L., Klump, J.V., 2011. Elemental and stable isotope records of organic matter input and its
37 fate in the Pichavaram mangrove-estuarine sediments (Tamil Nadu, India). *Mar. Chem.* 126, 163–172.
38 <https://doi.org/10.1016/j.marchem.2011.05.005>
- 39 Saad, Z., Kazpard, V., Geyh, M.-A., Slim, K., 2004a. Chemical and isotopic composition of water from springs and wells in the
40 Damour river basin and the coastal plain in Lebanon. *J. Environ. Hydrol.* 12.
- 41 Saad, Z., Slim, K., Khalaf, G., EL Samad, O., 2004b. Impacts des rejets des eaux résiduaires sur la qualité physico-chimique et
42 algologique du Nahr Antélias. *Bull. la Société neuchâteloise des Sci. Nat.* 127, 69–82.
- 43 Sahu, B.K., 1964. Depositional Mechanisms from the Size Analysis of Clastic Sediments. *J. Sediment. Petrol.* 34, 73–83.
- 44 Sanlaville, P., 1977. Étude géomorphologique de la région du littoral du Liban.
- 45 Schubert, C.J., Nielsen, B., 2000. Effects of decarbonation treatments on delta13C values in marine sediments. *Mar. Chem.* 72-,
46 55–59.
- 47 Sondi, I., Lojen, S., Juracic, M., Prohic, E., 2008. Mechanisms of land – sea interactions – the distribution of metals and sedimentary
48 organic matter in sediments of a river-dominated Mediterranean karstic estuary. *Estuar. , Coast. Shelf Sci.* 80, 12–20.
49 <https://doi.org/10.1016/j.ecss.2008.07.001>

- 1 Stevenson, F.J., Cheng, C.-N., 1970. Amino acids in sediments: Recovery by acid hydrolysis and quantitative estimation by a
2 colorimetric procedure. *Geochim. Cosmochim. Acta* 34, 77–88.
- 3 Tarabay, R., 2011. Vers un projet sociétal libanais ... L'environnement durable : une nouvelle citoyenneté ? Université Paris IV-
4 Sorbonne.
- 5 Thomas, R.L., Shaban, A., Khawlie, M., Kawass, I., Nssouli, B., 2005. Geochemistry of the sediments of the El Kabir River and
6 Akkar watershed in Syria and Lebanon. *Lakes Reserv. Res. Manag.* 10, 127–134.
- 7 Tselepidis, A., Polychronaki, T., Marrale, D., Akoumaniaki, I., Dell'Anno, A., Pusceddu, A., Danovaro, R., 2000. Organic matter
8 composition of the continental shelf and bathyal sediments of the Cretan Sea (NE Mediterranean). *Prog. Oceanogr.* 46, 311–
9 344.
- 10 Wang, C., Lv, Y., Li, Y., 2018. Riverine input of organic carbon and nitrogen in water-sediment system from the Yellow River estuary
11 reach to the coastal zone of Bohai Sea, China. *Cont. Shelf Res.* 157, 1–9. <https://doi.org/10.1016/j.csr.2018.02.004>
- 12 Wang, K., Chen, J., Jin, H., Li, H., Zhang, W., 2018. Organic matter degradation in surface sediments of the Changjiang estuary:
13 Evidence from amino acids. *Sci. Total Environ.* 637–638, 1004–1013. <https://doi.org/10.1016/j.scitotenv.2018.04.242>
- 14 Winogradow, A., Pempkowiak, J., 2018. Characteristics of sedimentary organic matter in coastal and depositional areas in the Baltic
15 Sea. *Estuar. Coast. Shelf Sci.* 204, 66–75. <https://doi.org/10.1016/j.ecss.2018.02.011>
- 16 Zhang, Q., Blomquist, J.D., 2018. Watershed export of fine sediment , organic carbon , and chlorophyll-a to Chesapeake Bay :
17 Spatial and temporal patterns in 1984 – 2016. *Sci. Total Environ.* 619–620, 1066–1078.
18 <https://doi.org/10.1016/j.scitotenv.2017.10.279>
- 19 Zhong, Y., Chen, Z., Li, L., Liu, J., Li, G., Zheng, X., Wang, S., Mo, A., 2017. Bottom water hydrodynamic provinces and transport
20 patterns of the northern South China Sea: Evidence from grain size of the terrigenous sediments. *Cont. Shelf Res.* 140, 11–
21 26. <https://doi.org/10.1016/j.csr.2017.01.023>
- 22 Zhu, C., Wang, Z., Xue, B., Yu, P., Pan, J., Wagner, T., Pancost, R.D., 2011. Characterizing the depositional settings for
23 sedimentary organic matter distributions in the Lower Yangtze River-East China Sea Shelf System. *Estuar. Coast. Shelf Sci.*
24 93, 182–191. <https://doi.org/10.1016/j.ecss.2010.08.001>

| | |
|---|----|
| Table 1: Description of sampling stations | 8 |
| Table 2: Linear discriminant functions to differentiate among environment of depositions | 11 |
| Table 3: Geochemical and biochemical results | 21 |
| | |
| Figure 1: A: Ibrahim River watershed and Dams location (Khalaf, 1984)..... | 7 |
| Figure 2: Sampling stations distribution at Ibrahim River coastal marine area..... | 9 |
| Figure 3: Grain size Class weight distribution (A), Mean vs Sorting (B), Mean vs Skewness (C), at the different sampling stations. | 16 |
| Figure 4: Ternary Diagram representing the grain size distribution (A) and the C-M Plot (B) for the sampling stations..... | 17 |
| Figure 5: Linear Discriminate Function (LDF) Plots (A: Y3 vs Y2, B: Y4 vs Y3) and spatial distribution of Y3 (C) at the studied area | 18 |
| Figure 6: Spatial distribution of OC (%) (A), TN (%) (B) and Mud (%) (C) at the Studied area.. | 20 |
| Figure 7: Chlorophyll spatial distribution (A) and Labile organic matter percentages (LOM) spatial distribution(B) at the studied area | 22 |
| Figure 8: $\delta^{13}\text{C}$ ranges and associated organic matter sources (A) and Spatial distribution of the terrestrial fraction (B) at Ibrahim River coastal marine area | 23 |
| Figure 9: Organic composition and grain size distribution in surface sediments A: Correlation Matrix (N=38 K=36 $r=0.324$, $p<0.05$; $r=0.418$, $p<0.01$; $r=0.518$, $p<0.001$) | 32 |

PCA - Biplot

